



**LTH**  
FACULTY OF  
ENGINEERING

Degree Project in Biotechnology - KBTM01

# Investigating recombinant transaminase stability with cofactor variations and enzyme immobilization

Moschopoulou Domniki

Supervisor: Eimantas Gladkauskas  
Assistant Supervisor: Andrius Jasilionis  
Examiner: Carl Grey

Spring 2024

## Popular Summary

Enzymes are nature's most versatile biocatalysts. These biomolecules act like tiny, specialized machines, each designed to perform a specific task with incredible precision and speed. In industrial processes, enzymes are important because they make chemical reactions happen faster and under milder conditions, saving energy and reducing the need for harsh chemicals. This makes the process like making medicines, cleaning products or even biofuels more effective, environmentally friendly and cost-effective. In drug development, the high specificity of the enzymes is used to produce the right structure of molecules that delivers the desired effect, as the mirror-image of that molecule can be harmful. One such enzyme important in the pharmaceutical industry is transaminase. Transaminases facilitate the transfer of amino groups between molecules. This simple reaction is particularly valuable to produce chiral amines, that can be found in more than 40% of pharmaceuticals.

However, like all machines, enzymes can sometimes be finicky, struggling with efficiency and durability, which has been the main obstacle so far to ditching harmful chemical processes. Particularly, transaminases struggle with stability and solubility. In simple terms, an enzyme needs to dissolve well in a solution (solubility) and maintain its structure and activity over time (stability) to be effective. If an enzyme precipitates out of solution or loses its function quickly, it becomes less useful, driving up costs and reducing efficiency in industrial processes. For that reason, a lot of research is devoted in improving the enzymes produced in model microorganisms.

Here, we tried to improve the stability of a transaminase isolated from the bacterium *Burkholderia multivorans* CDG1. This transaminase is particularly interesting for industrial use as it can maintain activity at very high temperatures and can be applied for a wide range of molecules. Firstly, we tried to improve stability by the addition of cofactor during the production of transaminase in the cell. Cofactors are small molecules that help enzymes in their tasks. We observed that adding the cofactor from the beginning of the enzyme production helped the enzyme to maintain their activity in a concentration-dependent manner. Another way to improve stability of enzymes is through immobilization. Essentially, the enzyme is attached to a surface or confined in a matrix in such a way that maintains its function and structure for a long time. This idea was applied to improve the stability and was successfully executed. However, more work needed to be done for the immobilization to be efficient enough, as many different parameters need to be optimized.

This work shows that different methods to improve stability are applicable but require further research to obtain efficient transaminase for chiral amine production.

## Preface

The master's degree project was carried out from 2024-01-22 to 2024-06-10 at Lunds Tekniska Högskola, Lund University, Faculty of Engineering, Department of Chemistry at the division of Biotechnology within the group of Bioorganic Chemistry.

Hypothesis of the project: The hypothesis of the project is that supplementing PLP during cultivation can increase the yield of soluble protein fraction for heterologous expressed amine transaminase.

Aim of the project: To evaluate concentration and supplementation time of PLP that improves the yield of the recombinant ATA-10 in the soluble protein fraction. An additional stabilization method of site-specific immobilizing the ATA-10 was explored on beads based on nickel affinity.

The main objectives were: 1. Evaluation of PLP toxicity towards cell growth. 2. Optimizing PLP supplementation conditions to increase the yield of the target protein in the soluble yield 3. Obtain the recombinant ATA-10 in pure solution. 4. Immobilization of the recombinant ATA-10 to improve stability for production processes.

## Acknowledgement

First, I would like to express my gratitude to my supervisors Eimantas and Andrius. To Eimantas, thank you for introducing me to the project and guiding me along the way. You trusted me and encouraged me along the way. To Andrius, thank you for sharing your vast wisdom and humour with me. I've learnt a lot about the complex world of recombinant protein expression. I also want to extend my gratitude to my examiner, Carl Grey, for always providing new perspectives and ideas during my time at the division. It was an enriching experience working alongside all of you and I hope to get the chance to work with you again in the future.

Moreover, I would like to thank the members of the Biorganic and Fermentation groups for welcoming me to their teams. I also want to thank everyone at the division of Biotechnology for all the fikas and puzzles and providing a pleasant environment. Lastly, I would like to share a big thanks to my friends and family (and my dog!) in Sweden and Greece for supporting me.

## Abstract

Amine transaminases are valuable biocatalysts in the pharmaceutical industry for the production of chiral amines. Their high regioselectivity and inherent regeneration of cofactor pose them as a greener alternative to the chemical synthesis. However, their application is hampered by their limited stability and narrow substrate scope and product inhibition. Recently, a stable tetrameric amine transaminase from *Burkholderia multivorans* CGD1, ATA-10, was identified and characterised. ATA-10 bears many characteristics attractive for industrial application. However, expression of ATA-10 by our group initially showed only poor recombinant expression in *Escherichia coli*.

In this work, the improvement of stability of the ATA-10 is examined. Firstly, supplementation of the co-factor, pyridoxal 5'-phosphate, was employed. Cultures with PLP supplementation at the beginning of the growth phase and before the induction phase at concentrations 0.01-1 mM were tested. Supplementation of the cofactor during cultivation didn't alter the target protein yield in the soluble protein fraction, which remained around 60% across all conditions. The effect of the cofactor was evident for the folding stability of the enzyme, as the activity was elevated when PLP was supplemented in the growth medium. This activity was linearly increased to the increase of PLP concentration, and the effect was more pronounced when PLP was added in the beginning of the culture. A potential inhibitory effect of high PLP concentrations was observed only during the induction phase, where 10 mM PLP resulted to halved growth. Highest activity was observed for ATA-10 produced in the presence of 1 mM PLP supplemented from the beginning of cultivation.

Purification of ATA-10 was achieved but complicated because of interference of PLP with the UV signal. To improve the stability of the ATA-10 for production processes, immobilization on hydrophilic carriers was carried out. Among the carriers, polyacrylic beads demonstrated higher immobilization yield and activity of the immobilized enzyme. Further optimization is required in order to apply the immobilization ATA-10 for chiral amines production.

## List of Abbreviations

<i>1-PEA</i>	1-phenylethylamine
<i>ACP</i>	Acetophenone
<i>ATA</i>	Amine transaminases
<i>ATA-10</i>	<i>Burkholderia multivorans</i> amine transaminase
<i>BA</i>	Benzyl acetone
<i>BSA</i>	Bovine serum albumin
<i>HCl</i>	Hydrochloric acid
<i>HPLC</i>	High pressure liquid chromatography
<i>IDA</i>	Iminodiacetic acid
<i>IMAC</i>	Immobilised metal affinity chromatography
<i>IPA</i>	Isopropylamine
<i>IPTG</i>	isopropyl $\beta$ -D-1-thiogalactopyranoside
<i>LB-Lennox</i>	Lysogeny broth Lennox
<i>MPPA</i>	1-methyl-3-phenylpropylamine
<i>MW</i>	Molecular Weight
<i>OD<sub>600</sub></i>	Optical density measured at 600 nm
<i>PLP</i>	Pyridoxal 5'-Phosphate
<i>PMP</i>	Pyridoxamine 5'-phosphate
<i>RT</i>	Room temperature
<i>SDS-PAGE</i>	Sodium dodecyl sulphate polyacrylamide gel electrophoresis
<i>SF</i>	Soluble protein fraction
<i>TAs</i>	Transaminases
<i>Tris</i>	tris(hydroxymethyl)aminomethane

## Table of Contents

Popular Summary .....	2
Preface .....	3
Acknowledgement.....	4
Abstract .....	5
List of Abbreviations .....	6
1. Introduction .....	9
1.1. Pyridoxal 5' – phosphate dependent enzymes .....	9
1.2. Transaminases .....	9
1.2.1. Classification.....	9
1.2.2. Challenges of transaminases as biocatalysts .....	10
1.2.3. Immobilization of TAs to enhance stability .....	11
1.2.4. ATA-10, a highly stable transaminase from <i>Burkholderia multivorans</i> .....	11
1.3. Recombinant protein expression .....	12
2. Material and Methods.....	13
2.1. Strains, vectors, media, and chemicals.....	13
2.1.1. Heat-shock transformation .....	13
2.2. Production of recombinant ATA-10 transaminase.....	13
2.2.1. Cultivation and heterologous expression .....	13
2.2.2. Protein extraction for analysis.....	14
2.2.3. Protein purification with immobilized metal affinity Chromatography (IMAC) 14	
2.2.4. Protein concentration measurement with Bradford method.....	14
2.2.5. Sodium dodecyl sulphate polyacrylamide gel electrophoresis and protein densitometry .....	15
2.2.6. Enzyme activity assay .....	15
2.3. Immobilization of ATA-10 .....	16
2.3.1. Degree of ATA-10 binding calculations .....	17
2.3.2. Estimating immobilized ATA-10 activity in two-phase reaction system .....	18
3. Results and Discussion.....	20
3.1. Initial test of recombinant protein expression without PLP .....	20
3.2. Expression of ATA-10 at a variable concentration of pyridoxal-5' -phosphate ...	20

3.2.1.	Purification of ATA-10 from soluble protein fraction .....	24
3.2.2	Testing limits of PLP supplementation.....	25
3.3.	Immobilization – Stability of enzyme .....	27
3.3.1.	Initial screening of beads.....	27
3.3.2.	Testing different immobilization conditions .....	31
4.	Conclusions .....	33
5.	References .....	35
6.	Appendix .....	40



## 1. Introduction

### 1.1. Pyridoxal 5' – phosphate dependent enzymes

Pyridoxal 5'–phosphate dependent enzymes are a diverse group of enzymes primarily involved in the biosynthetic pathways of amino acids and their derived metabolites and other amine-containing compounds (Eliot and Kirsch, 2004). These enzymes use pyridoxal 5'–phosphate (PLP), one of the active forms of vitamin B<sub>6</sub>, as a cofactor. PLP activates the enzymes through a transaldimination step. Firstly, PLP covalently binds to a highly conserved lysine residue in the active center forming the internal aldimine, which is the catalytically active state of the enzyme (Oliveira et al., 2011). When the substrate is present it reacts with the PLP-enzyme complex and then the bond with the Lys is displaced and a new aldimine is created between the PLP and the substrate (external aldimine). The following reaction depends on the enzyme and the type of substrate (John, 1995).

For that reason, PLP-dependent enzymes have a vast catalytic variety including racemization, decarboxylation, transamination, beta elimination among others. That renders them as attractive biocatalysts for industrial purposes, owing to their high regio and stereo-selectivity (Rocha et al., 2019). Structurally, PLP-dependent enzymes are categorized in 7 different fold types (Grishin et al., 1995, Percudani and Peracchi, 2009). These fold types are composed of enzymes catalyzing diverse kinds of reactions.

### 1.2. Transaminases

Transaminases (EC 2.6.1), also known as aminotransferases, are PLP-dependent enzymes responsible for the transference of an amino group from an amino acid to  $\alpha$ -keto acids. In that way, their role in nitrogen metabolism and biosynthetic pathways of amino acids is crucial.

The reaction mechanism of TAs can be considered as two half-reactions, where PLP acts as a shuttle of the amine group (**Figure 1**). With the amine donor present, the external aldimine is formed replacing the bond with the lysine in the active site. The aldimine is deprotonated at the C $\alpha$  of the substrate, which leads to a quinonoid intermediate. Reprotonation and hydrolysis yields the keto-acid byproduct and the non-covalently bound aminated cofactor pyridoxamine-5'-phosphate (PMP). The proton transfer is promoted by the conserved Lys (Toney and Kirsch, 1993) and the quinonoid state is stabilized by uncharged aromatic amino acids (Toney, 2005). Essentially, the reverse mechanism is followed for the second half reaction, where the amine group is transferred from PMP to the amine acceptor, a ketone, yielding the corresponding amine and the regenerated internal aldimine (Liang et al., 2019).

#### 1.2.1. Classification

As PLP-dependent enzymes, transaminases belong to the fold-type I and fold-type IV. Fold-type I, also referred to as the aspartame aminotransferase family, contains the majority of the

transaminases which are also classified by their sequence similarity in 5 classes. Fold-type IV contains the D-alanine aminotransferases and branch-chain aminotransferases and are considered the 6<sup>th</sup> class of transaminases (Grishin et al., 1995). Another common classification of transaminases is done based on the substrate and can be divided into two groups:  $\alpha$ -transaminases ( $\alpha$ -Tams) and  $\omega$ -transaminases ( $\omega$ -Tams).  $\alpha$ -Tams require the presence of a carboxylic group in the  $\alpha$ -position with respect to carbonyl functionality and hence forming only  $\alpha$ -amino acids (Höhne and Bornscheuer, 2009).  $\omega$ -Tams include all the other transaminases and can accept aliphatic ketones and amines, which has increased their appeal for industrial purposes. All  $\omega$ -Tams belong to Class III (Fold-type I) and can be further distinguished into two subgroups,  $\beta$ -transaminases ( $\beta$ -Tams) and amine transaminases (ATA) (Kelly et al., 2017).

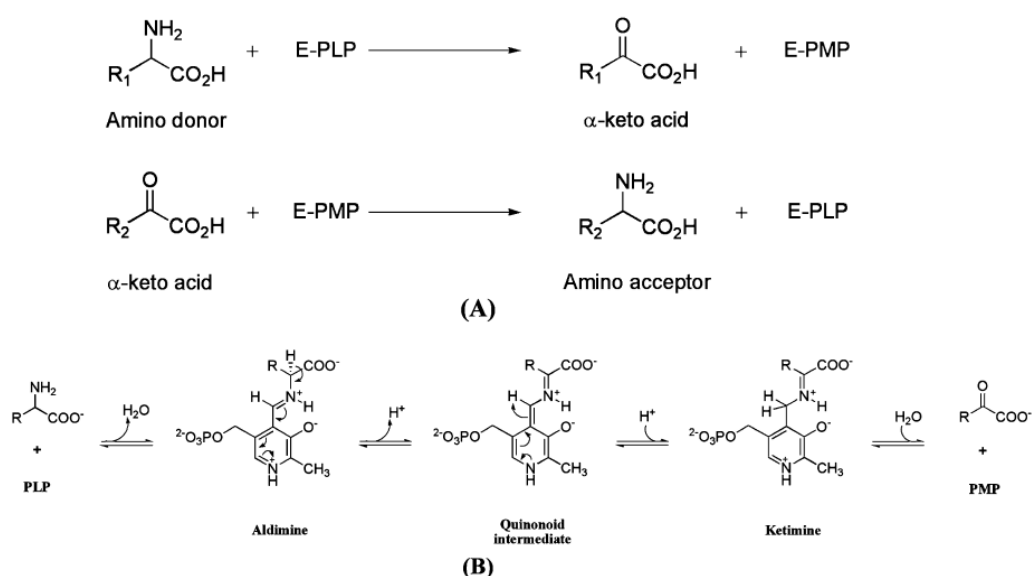


**Figure 1 Transamination reaction mechanism.** A: The reaction can be considered as two half reactions. B: The different states of cofactor pyridoxal 5'-phosphate (PLP) during transamination (Mathew and Yun, 2012)

### 1.2.2. Challenges of transaminases as biocatalysts

As a biocatalyst, TAs offer a greener alternative for the stereoselective amination of prochiral ketones. Their high regioselectivity and inherent regeneration of the cofactor and their mild operating conditions render them promising biocatalysts for chiral amine production. The chiral amines are valuable building blocks in the pharmaceutical industry. It is estimated that 40% of all pharmaceuticals contain a chiral amine component (Ghislieri and Turner, 2013). Production of chiral amines can be achieved in two ways with  $\omega$ -TAs, kinetic resolution of a racemate and asymmetric synthesis, the latter of which has a theoretical yield of 100% (Koszelewski et al., 2010b).

However, the wide application of  $\omega$ -TAs as biocatalysts is impeded by product/substrate inhibition, narrow substrate scope and poor stability. Several strategies have been employed to counteract these drawbacks. The physical removal of the product and the use of isopropylamine

(IPA), a low molecular weight amine donor have led to significant improvements in the product inhibition (Savile et al., 2010). Protein engineering of  $\omega$ -TAs has proved to be an invaluable tool to not only broaden the substrate scope but also overcome the substrate inhibition (Cho et al., 2008). The most successful example of pharmaceutical compound industrially produced by engineered  $\omega$ -TAs is the antidiabetic drug sitagliptin. An engineered (R)-selective  $\omega$ -TAm ATA-117 from *Arthrobacter* sp. was developed that led to a drastic increase in yield (10–13%) and productivity (53%, measured in kg L<sup>-1</sup> per day), while reducing the total waste by 19% and eliminating the need for heavy metals at the same time (Savile et al., 2010).

### 1.2.3. Immobilization of TAs to enhance stability

Stability of biocatalysts is crucial for industrial applications. TAs are characterized by limited stability that occurs when PLP is dissociated from the enzyme (apoenzyme). The apoenzyme is the least stable form of the TAs and prone to aggregation (Börner et al., 2017). Different stabilization methods have been explored, such as protein engineering, reaction medium engineering and biocatalyst formulation. Immobilization is a practical and economical strategy for industrial biocatalysts as it allows the recycling of the catalyst even though it usually leads to lower enzyme activity (Mallin et al., 2014). Chitosan is the most common carrier used for immobilization of TAs. The commercial  $\omega$ -TA from *Vibrio fluvialis*, VfTA was covalently immobilized on chitosan beads and resulted in high operational (retention up to 77% of activity after 5 repetitive uses) and storage stability (70% of initial activity after 3.5 weeks storage at 4 °C) (Yi et al., 2007). (R) and (S)- selective  $\omega$ -TAs were also successfully immobilized on chitosan with glutaraldehyde linker that resulted in higher thermostability of the bound enzymes and higher conversions compared to the free enzyme (Mallin et al., 2014). Whole cell immobilization of *E. coli* cells containing  $\omega$ -TA has also been studied before (Rehn et al., 2012). Other preparations on as sol-gel (Koszelewski et al., 2010a), glass beads (Engelmark Cassimjee et al., 2014) or cellulose (de Souza et al., 2016) have yielded more  $\omega$ -TAs with improved stability.

### 1.2.4. ATA-10, a highly stable transaminase from *Burkholderia multivorans*

Recently, a very stable transaminase was identified and characterized by Kollipara et al., 2022. ATA-10 from *Burkholderia multivorans* CGD1 (B9AZ94) belongs to the new functional subfamily of  $\beta$ -alanine:pyruvate TA, with parent enzyme TA-3N5M characterized by the same group. TA-3N5M belongs to the class III Fold I transaminases but differs from other amine transaminases (ATA). Members of the TA-3N5M subfamily lack the conserved “flipping” arginine residue, but instead carries an alternative dual substrate recognition characterized by R162. Although it has a relatively narrow amine substrate range, it accepts  $\beta$ -alanine,  $\gamma$ -amino butyric acid and other  $\omega$ -amino acids, 1-phenylethylamine (1-PEA) and isopropylamine as amino donors and pyruvate as amino acceptor (Steffen-Munsberg et al., 2016). Both TA-3N5M and other members of the family form tetramers which have been previously associated with higher protein stability (Börner et al., 2017).

ATA-10 was indeed found to bear the ATA-typical “flipping” arginine (R346) but also forming tetramers owing to the high global sequence identity to TA-3N5M. Its sequence also bears residues (W47 and A185) associated with highly active ATAs. ATA-10 accepts a variety of aliphatic small and larger ketones but prefers 1-PEA and pyruvate as ideal amino donor and acceptor respectively. TA-10 shows high thermostability up to 70 °C for both resting (75% residual activity) and operating conditions (50% residual activity). In addition, ATA-10 is highly resistant to commonly used organic solvents such as DMSO, methanol and isopropanol even at elevated concentrations (up to 50% at 30 °C and up to 25% at 60 °C) (Kollipara et al., 2022). All these characteristics pose ATA-10 as an interesting highly active and stable candidate for chiral amine synthesis.

### 1.3.Recombinant protein expression

Recombinant DNA technology had been a catalyst for the expansion of biotechnology applications. The most common recombinant cell factory employed is *Eschericia coli* owing to its relative simplicity, its inexpensive and fast high-density cultivation, the well-known genetics and the large number of compatible molecular tools available. Despite all this merits, recombinant protein expression is usually complicated by insoluble or nonfunctional proteins. Strategies to improve solubility include optimizing cultivation conditions, reducing temperature, using chaperones, and co-expressing proteins with specific tags (“solubility tags”) (Sørensen and Mortensen, 2005).

Another approach is the supplementation of cofactor to the growth medium. Many cofactors have stabilization effects on the respective enzyme, promoting the correct conformation. Adding 1 µM of riboflavin 2 h before induction during the expression of FAD-containing protoporphyrinogen oxidase increased the amount of the recovered enzyme by approximately 4-fold. This effect is realised by the presence of riboflavin transmembrane import system *E. coli* (Atroshenko et al., 2024). The soluble protein expression of the PLP-dependent O-acetylserine sulphdrylase (OASS) of *H.contortus* was increased when PLP was added during cultivation. More specifically, PLP concentrations of 0.01 to 0.1 mM led to linear increase in the soluble protein expression yield. Moreover, this study demonstrated the potential uptake of PLP from *E.coli* by tryptophan quenching assay, and that uptake was correlated with the increase soluble expression (Saxena et al., 2022).

So far, supplementation of PLP has been mainly associated with increasing the specific enzymatic activity. The addition of 0.02 mM of pyridoxal phosphate (pyridoxine-5-phosphate) increased the yield of active glutamate decarboxylase by 2–2.5 times and simultaneously double increased in glutamate decarboxylase specific activity (Plokhov et al., 2000). At the same time, the non-phosphorylated form, pyridoxine allows for increase in yield and stability of the active glutamate decarboxylase, while increased 1.5-fold the specific activity when supplemented at concentrations above 0.05 mM (Huang, Su and Wu, 2016).

## 2. Material and Methods

### 2.1. Strains, vectors, media, and chemicals

*Escherichia coli* BL21 (DE3) strain ( $F^- ompT gal dcm lon hsdSB(r_B^- m_B^-) \lambda(DE3 [lacI lacUV5-T7 gene 1 ind1 sam7 nin5])$ ) (Merck) was used for heterologous production. The ATA-10 amine transaminase gene from *Burkholderia multivorans* CGD1 (UniProtKB UB9AZ94) with a C-terminal hexa-his-tag was cloned via *NdeI* and *XhoI* restriction into pET-22b(+) (Merk) vector ordering *de novo* synthesis of codon non-optimized gene sequence (BioCat). Lysogeny broth (LB)-Lennox medium (Difco BD) was used for cultivation supplemented with 100  $\mu\text{g}/\text{mL}$  ampicillin if necessary solidifying media with 2% (w/v) bacteriological agar-agar (Saveen Werner). The pET-22b(+) vector without any insert was used as a positive control for the transformation. Pyridoxal 5'-phosphate (PLP) monohydrate was purchased from Sigma-Aldrich (Merck) and isopropyl  $\beta$ -D-1-thiogalactopyranoside (IPTG) was supplied by PanReac AppliChem (ITW Reagents).

#### 2.1.1. Heat-shock transformation

The expression construct or empty vector were transformed applying the heat-shock method. After thawing the 25  $\mu\text{L}$  competent cells and DNA samples on ice, 1  $\mu\text{L}$  with approximately 6 ng of DNA samples was transferred and gently mixed with competent cell suspension. The contents were further mixed gently by flicking the bottom of the tube a few times and then incubated on ice for 30 min. Heat-shock at 42  $^{\circ}\text{C}$  for 60 s was applied, before transferring the tubes back on ice for another 15 min. 100  $\mu\text{L}$  of room temperature SOC were added into the mixture that was then mixed gently by pipetting. Approximately 50  $\mu\text{L}$  of the transformed suspension was plated in LB-Lennox agar plates containing 100  $\mu\text{g}/\text{mL}$  ampicillin and the cells were incubated for at 37  $^{\circ}\text{C}$  at 16 h. After cultivation plates were inspected evaluating size as well as morphology of colonies.

## 2.2. Production of recombinant ATA-10 transaminase

### 2.2.1. Cultivation and heterologous expression

The cultivation protocol of the recombinant ATA-10 transaminase was based on the study of Kollipara et al., 2022. The cultivation can be distinguished in two phases: the growth and the production phase. Fresh inoculum was prepared the day before from single colonies spread on LB-Lennox agar plates containing ampicillin and incubated at 37  $^{\circ}\text{C}$  overnight until fully seeded. The preculture was collected in a conical tube with 58 mL fresh LB-Lennox, when the optical density at 600 nm ( $\text{OD}_{600}$ ) was measured. 250 mL cultures with a starting  $\text{OD}_{600}$  of 0.06 were carried out in 1 L baffled shake flasks by inoculating up to 1 % (v/v). The growth phase continued at 37  $^{\circ}\text{C}$  at 140 rpm until the culture reached  $\text{OD}_{600} \sim 0.6$ . Then the production of the recombinant ATA-10 was induced at preequilibrated 20  $^{\circ}\text{C}$  by supplementing culture with 1 mM of freshly prepared IPTG for 20 h.  $\text{OD}_{600}$  measurements were taken throughout the growth phase and before harvesting to monitor cell growth. Upon completion of the induction phase,

the cells were harvested by centrifugation at  $8000\times g$  at  $4\text{ }^{\circ}\text{C}$  for 20 min. The supernatant was discarded, and the cells were kept in  $-20\text{ }^{\circ}\text{C}$ .

To examine the effect of PLP on the expression and the activity of the recombinant ATA-10, 3 different concentrations and two different supplementation schemes were examined. PLP concentrations of 0.01, 0.1, and 1 mM were supplemented at the beginning of the cultivation ( $t_{(0)}$ ) or 20 min before induction ( $t_{(i)}$ ). Moreover, 10 mM PLP supplemented at  $t_0$  was also tested to examine limitations of PLP toxicity. A control culture without PLP was run in all cases, to detect any possible effects of the PLP toxicity on the bacterial growth or protein solubility.

#### 2.2.2. Protein extraction for analysis

Frozen cell pellets were thawed on ice and resuspended in the lysis buffer (50 mM HEPES-NaOH pH 7.4, 500 mM NaCl, 50 mM imidazole and 10 % (v/v) glycerol) were sonicated using the Ultrasonic Liquid Processor (Fisherbrand). 8-12 mL of bacterial suspension was sonicated for 15 minutes at 40% amplitude and 0.5 cycle (30 s pulse: 30 s pause). Samples were kept on ice while sonicated to prevent heating and protease degradation. To collect the soluble protein fraction where ATA-10 is expected to be present, the lysate was centrifuged using the same centrifuge at  $17000\times g$  for 20 min at  $4\text{ }^{\circ}\text{C}$  and the supernatant was collected. The soluble protein fraction was kept for further analysis. Samples from both total and soluble protein fraction were collected to evaluate the soluble content with SDS-PAGE analysis (see 2.2.5).

#### 2.2.3. Protein purification with immobilized metal affinity Chromatography (IMAC)

Nickel affinity chromatography was used to purify the ATA-10 transaminase using HisTrap HP 1 mL column (Cytiva) with ÄKTA start FPLC purification system (GE Healthcare Life Sciences). The binding to resin of target protein was performed in the lysis buffer conditions and elution buffer contained 50 mM HEPES-NaOH, 500 mM NaCl, 500 mM imidazole and 10 % (v/v) glycerol. The samples were filtered using a  $0.2\text{ }\mu\text{m}$  regenerated cellulose filter (GE Healthcare Life Sciences) prior to loading onto column. Target proteins were eluted by single step elution after extensive column washing with 8 column volumes (CV) with lysis buffer. It should be noted that the selected PLP concentration surrounding the target protein remained constant throughout the lysis and well as purification. For that reason, both lysis and elution buffer were supplemented with the same concentration of PLP as of the culture of the pellet analysed.

#### 2.2.4. Protein concentration measurement with Bradford method

The protein concentration in soluble protein fraction and after purification was measured applying the Bradford protein assay (Compton and Jones, 1985). The Bradford assay solution (ready-to-use) (TCI Chemicals) was used for this purpose. The reagent contains Coomassie Brilliant Blue G-250 dye in an acid environment in its cationic state, absorbing at 620 nm. Upon



binding to protein, Comma<sup>s</sup>sie Brilliant Blue G-250 enters its anionic state, absorbing at 595 nm. The absorbance at 595 nm is thus proportional to the protein concentration.

The assay was carried out by mixing 1 mL of the Bradford reagent with 25  $\mu$ L of the sample or the standard in a cuvette. The mixture was incubated at room temperature for 5 min, after which the absorbance was measured spectrophotometrically at 595 nm. A calibration curve was created with bovine serum albumin (BSA) (Pierce Bovine Serum Albumin Standard Ampules, 2 mg/mL, Thermo Fisher Scientific) as standard. Using the lysis buffer, BSA dilutions of 0, 0.05, 0.1, 0.25, 0.5, 0.75, 1.0, and 1.2 were prepared. As blank 25  $\mu$ L of binding buffer were used. In the case of PLP-containing samples, the respective PLP-containing binding buffer was used.

Absorbance at 280 nm was also tested aiming to measure protein concentration but proved to be non-linear for samples containing PLP since the latter compound absorption range is also including 280 nm (see Figure 13, Appendix).

#### 2.2.5. Sodium dodecyl sulphate polyacrylamide gel electrophoresis and protein densitometry

7.5 % glycine-SDS-PAGE was performed using a Mini-PROTEAN Tetra Cell electrophoresis system (Bio-Rad). Samples were prepared by adding 4x Laemmli Sample buffer (Bio-Rad) supplemented with  $\beta$  mercaptoethanol obtaining final dye:sample ration of 1:3. The tubes were mixed by vortexing and stored at 4 °C until analysis. The samples were heated at 100 °C for 10 min and then spin-down before loading on the gel. Mini-PROTEAN TGX Stain-Free precast gels (Bio-Rad) were used for electrophoresis, loading gel) with 6-10  $\mu$ L of sample loaded in each lane along with 7  $\mu$ L of Precision Plus Protein Standards protein ladder (Bio-Rad). The electrophoresis was performed at 15 V/cm. Electrophoretic profiles were visualized with GelDoc GO Imaging System (Bio-Rad). The target enzyme relative presence in electrophoretic profile of the soluble protein fractions was estimated with densitometry using Image Lab Touch v3.0 Software (Bio-Rad).

#### 2.2.6. Enzyme activity assay

The enzyme activity of the recombinant ATA-10 was evaluated by the acetophenone assay. The substrate used for the assay contains 40 mM 1-phenylethylamine (1-PEA) pH 8, 40 mM pyruvate, 2 mM PLP, 150 mM Tris and 10% (v/v) glycerol. In the presence of transaminase, the 1-phenylethylamine acts as the amine donor and pyruvate as the amine acceptor catalysing the reaction shown in Figure 2. The formation of acetophenone over time can be monitored by measuring the absorbance at 250 nm. For the assay, in a UV-suitable cuvette 50  $\mu$ L of the substrate is mixed with 10-100  $\mu$ L sample and ultrapure (Milli-Q grade) water until final volume reaches 1 mL. After the components are well mixed by pipetting, the absorbance at 245 nm is monitored over 5 min. The slope of the graph  $AU=f(t)$  equals the rate of activity. Using known samples of ACP a standard curve was created. In that way the rate is converted to

the rate of mM ACP produced/min. The specific activity is calculated by dividing the rate of mM ACP produced/min with the ug of total protein in the sample.

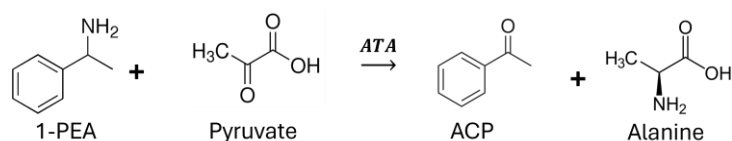


**Figure 2 Reaction mechanism of the acetophenone detection assay.** 1-Phenylethylamine (1-PEA) acts as the amine donor and pyruvate as the amine acceptor. In the presence of a transaminase pyruvate gets aminated forming alanine and the acetophenone (ACP). The conversion of ACP is monitored by absorbance at 250 nm.

### 2.3. Immobilization of ATA-10

To be able to explore the applicability of the recombinant transaminase in reaction systems, an immobilization method based on nickel affinity was employed. Two different beads, IB-HIS-2 and IB-HIS-22, that both have nickel attached by iminodiacetic acid (IDA) were supplied by ChiralVision. The specifications of the two carriers are presented in **Table 1**.

**Table 1 Immobilization carriers characteristics.**

Carrier	Type	Matrix	Functional group	Water content (%)	Bead size ( $\mu\text{m}$ )	Ni loading (dry) mol/g
IB-HIS-2	hydrophilic	Polyacrylic acid	IDA-Ni, low butyl	75	150-710	30
IB-HIS-22	Extremely hydrophilic	Cellulose	IDA-Ni	50	20-40	97

For screening purposes, the immobilisation was carried out in micro-scale, for which 100 mg beads should be mixed with 400  $\mu\text{L}$  of enzyme solution of 10-100 mg protein/mL under supplier's guidelines. 50 mg beads were mixed with adequate volume of clarified lysate to ensure a ratio of  $\sim 20$  ug enzyme/mg beads estimating target enzyme concentration in the soluble protein fraction by combining concentration and densitometry measurements. The tubes were shortly vortexed and then incubated at room temperature (RT) on a nutator plate for 2 minutes. Following that the immobilization took place either at 4  $^{\circ}\text{C}$  or RT, statically or stirred on a nutator plate, for 3 or 40 h.

After the immobilization, the immobilization mix was separated into beads and non-immobilized fraction by 2 min spin-down centrifugation (Centrifuge 5424 R, Eppendorf). non-immobilized fraction, the fraction containing the non-immobilized protein, was kept for analysis. Both total protein concentration and enzyme activity assays were performed using the non-immobilized fraction following the calculations explained in section 2.3.1. The collected beads were washed 5 times with 1 mL ultrapure Milli-Q water by centrifugation at max speed for 2 min. The supernatant was collected carefully by pipetting to avoid loss of beads.



### 2.3.1. Degree of ATA-10 binding calculations

To determine the degree of ATA-10 binding the immobilization yield and activity yield after immobilization were calculated. Using the Bradford assay, the collected non-immobilized fraction was used to estimate the total protein concentration after immobilization ( $C_{total,after}$ ). The total amount of protein bound on the carrier can be calculated by the differences in the total protein concentration before and after the immobilization:

$$P_{bound} = (C_{total,before} - C_{total,after}) * V_{lysate}$$

The initial free enzyme amount ( $ATA10_{free, initial}$ ) is calculated by combining the Bradford method and densitometry (see sections 2.2.4 and 2.2.5). The lysates used contain recombinant ATA-10 and 50 mM imidazole, that both have affinity to the bound nickel on the beads' surface. Although the imidazole binding on  $Ni^{2+}$  residues cannot be quantified, the concentration is quite low that allows proper interaction between the his-tag protein and the nickel on the chromatography resins. Thus, the imidazole binding is considered negligible, and it is assumed that all bound protein on the carrier corresponds to recombinant ATA-10, *i.e.*:

$$P_{bound} = ATA10_{bound}$$

Thus, the immobilization yield can be calculated as the ratio of the bound enzyme to the initial free enzyme amount, expressed as a percentage.

$$Immobilisation\ yield\ (\%) = \frac{ATA10_{bound}}{ATA10_{free, initial}} * 100\%$$

In the same manner, the activity yield was also estimated. The specific activity of the enzyme before immobilization *Specific activity*<sub>free enzyme</sub> (*mM ACP/min/ug total protein*) is calculated as explained in section 2.2.6. Using the ACP assay the enzyme activity of the non-immobilized fraction was estimated. The specific activity of the non-immobilized fraction (*Specific activity*<sub>non-immobilized</sub>) was calculated using the measured  $C_{total,after}$ . The specific activity of the bound protein (*i.e.* bound ATA-10) can be calculated as the difference between the specific activity of the free enzyme and the non-immobilized fraction:

$$Specific\ activity_{bound} = Specific\ activity_{free\ enzyme} - Specific\ activity_{non-immobilized}$$

Following the same assumption that all bound protein responds to the bound ATA-10, the activity yield can be calculated as the ratio of the specific activity of the bound enzyme to the specific activity of the initial free enzyme, expressed as a percentage.

$$Activity\ yield\ (\%) = \frac{Specific\ activity_{bound}}{Specific\ activity_{free\ enzyme}} * 100\%$$

### 2.3.2. Estimating immobilized ATA-10 activity in two-phase reaction system

To test the activity of the immobilized ATA-10 a two-phase reaction system was used. This reaction includes the transamination of isopropylamine (Sigma Aldrich) to 1-methyl-3-phenylpropylamine with benzyl acetone (TCI Chemicals) as the amine acceptor. The reaction is presented in Figure 3.

The substrate buffer used for the reaction contains 500 mM IPA pH 8, 2 mM PLP, 150 mM Tris-NaOH and 10% v/v glycerol. The washed beads were resuspended in 3 mL of the substrate buffer and transferred to 5 mL glass vials. Then, 50  $\mu$ L of BA was added to start the reaction. The vials were continuously stirred at 700 rpm at 30 °C on a thermoshaker (Hettich). 100  $\mu$ L samples were taken before (time 0 of reaction) and 1, 4, 19 and 91 h after the addition of BA transferred to HPLC vials containing 400  $\mu$ L of HCl 0.1 mM to stop the reaction. The samples were stored at 4 °C until analysis with HPLC.

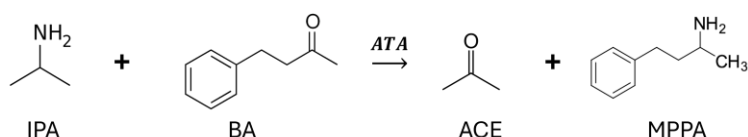


**Figure 3** Reaction mechanism of conversion of isopropylamine (IPA) to 1-methyl-3-phenylpropylamine (MPPA) with benzyl acetone (BA) as the amine donor in a two-phase system.

The chromatographic detection of the MPPA formation was conducted using high-performance liquid chromatography (HPLC) as described by Börner et al., 2016. HPLC system details are presented in Table 2. All relevant reaction components were analysed (1  $\mu$ L injection sample) by reverse phase chromatography using a Kinetex 2.6  $\mu$ m EVO C18 100 Å column (Phenomenex). The reaction components were separated in isocratic mode with mobile phase containing 35% acetonitrile and 65% ultrapure Milli-Q H<sub>2</sub>O at pH 11.5 with a flowrate of 0.45 mL/min. MPPA eluting at 1.7 min and BA eluting at 2.2 min were detected with UV/Vis detection at 260 nm at 30 °C. Quantification was made from a calibration curve with standard solutions of BA and MPPA described in Table 3.

**Table 2** HPLC equipment specifications.

Equipment	Model
Autosampler	Dionex UltiMate 3000 Autosampler
UV/ Visible Detector	Dionex UltiMate 3000 Diode Array Detector
Column	Dionex UltiMate 3000 Column compartment
Pump	Dionex UltiMate 3000 RS Pump

*Table 3 Standard solutions used for quantification through a calibration curve.*

<b>Standards</b>	<b>Concentration (mM)</b>							
<b>BA</b>	0.25	0.50	1.00	2.00	4.00	8.00	9.00	10.00
<b>MPPA</b>	0.39	0.78	1.56	3.12	6.12	12.5	25.00	50.00

### 3. Results and Discussion

#### 3.1. Initial test of recombinant protein expression without PLP

To assess the baseline expression, the recombinant transaminase was produced without the addition of PLP cofactor, following the expression protocol described by Kollipara et al., 2022. The enzyme was successfully expressed in *E. coli* BL21(DE3) cells with a final OD<sub>600</sub> ~ 3. Highlighted in the Figure 4A is the recombinant ATA-10 with theoretical MW 48.8 kDa. Although the ATA-10 is overexpressed in the host cells, it appears that only a small amount of it remained in the soluble protein fraction (approximately 20% of total fraction). Analysis of the band intensity of protein electrophoresis gel gave a yield of the target protein in the soluble protein fraction of 23.7%. Purification of the enzyme from the rest of the soluble proteins proved successful with a final concentration of the enzyme at 1,26 mg/mL. Following the analysis, the purified ATA-10 was stored at 4 °C where aggregation was observed after 3 days (Figure 4B). These initial results showed that ATA-10 can be successfully expressed in *Escherichia coli* following the current protocol, but the stability of the enzyme needs to be further improved.

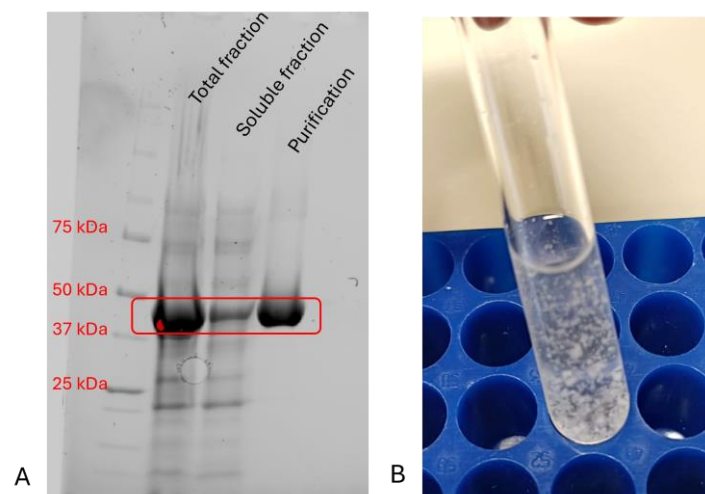


**Figure 4** Screening test of baseline ATA-10 production in *E. coli* BL21(DE3) cells. A: SDS-PAGE of samples after extraction and purification. 1 lane: As a protein molecular mass standard the Precision Plus Protein (Biorad) was used, 2 lane: sample from total fraction after cell lysis. 3 lane: sample from soluble protein fraction collected and 4 lane: sample after purification of the sample. It can be seen here that the expression yield of the recombinant protein is quite high, with the soluble protein fraction representing about 20% of the total one. ATA-10 represents 23.7% of the soluble protein fractions. A first round of purification was also successful yielding 1.26 mg/mL pure enzyme. B: Pure enzyme after 3 days storage at 4°C. Severe aggregation can be observed directly.

#### 3.2. Expression of ATA-10 at a variable concentration of pyridoxal-5'-phosphate

Based on the findings of Saxena et al., 2022, supplementation of PLP can aid the expression of recombinant PLP-dependent enzymes. For that reason, cultures of *E. coli* BL21 (DE3)

containing the ATA-10 construct with supplementation of PLP at two different time points were carried out. The cultures were carried out in duplicates (Figure 5).

Only small changes in cell growth were observed when the growth media was supplemented with PLP concentrations of 0.01 to 1 mM (Figure 5). Until induction the OD of the cultures is quite similar, but differences only occur after the induction of protein expression. In both replicates, the final OD at time of harvest ranges between 4.0 and 5. An exception to this is the culture with 1 mM PLP supplemented at  $t_{(0)}$  with a final OD of 3.5. This is likely to errors during inoculation that led to slower starting OD. However, in both replicates the supplementation of PLP at 1 mM at the start of the cultivation leads to slower growth until induction than the no PLP one. Combined with the fact that these cultures have the lowest OD at time of harvest, it could indicate that PLP at higher concentrations could have an inhibitory effect to the cell growth. On the other hand, cultures with 0.01 mM PLP independently to the time of addition demonstrate higher or similar cell growth during growth and induction phase than no PLP. These observations imply that PLP at low concentrations has no inhibitory or even stimulating effect on the cell growth, in contrast to 1 mM PLP.

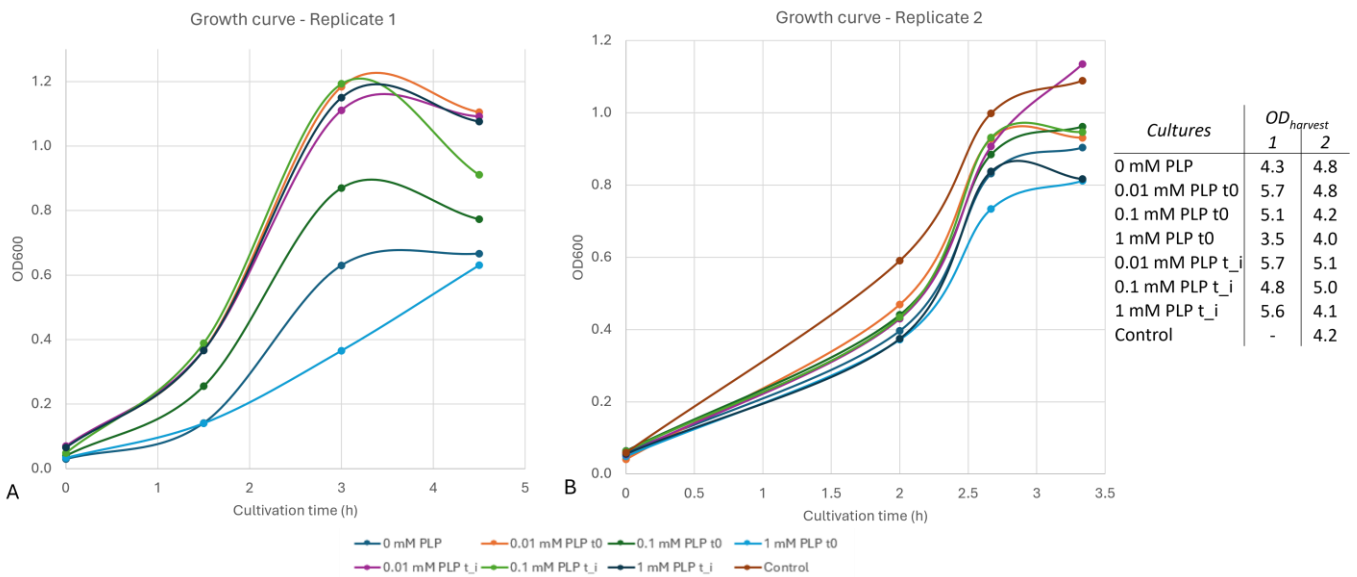


**Figure 5 Growth curves of cultures with PLP supplementation until induction with 1 mM IPTG.** A: Results from the first replicate. The OD<sub>600</sub> of induction varies in this case from 0.6 to 1.1. However, the final OD<sub>600 nm</sub> is around 3.5 to 5.7. Here it should be noted that the culture where 1 mM PLP was supplemented from the beginning has smaller growth than the control probably due to smaller inoculum. 0.01 mM PLP shows higher cell growth than the control independently of the time of addition. B: Results from the second replicate. An additional control without induction was carried out too. Here the growth until induction seems to be more in unison. Again, 1 mM PLP  $t_{(0)}$  has slightly smaller growth than no PLP, while 0.01 and 0.1 mM PLP show a slightly higher growth. At harvesting the cultures can be distinguished in two different groups. The one with higher final OD<sub>600</sub> of 5 that includes the 0 mM PLP and 0.01 mM PLP at either time of addition and 0.1 mM PLP at time of induction. The other group had a slightly lower growth (final OD 4.0-4.2) and contains both 1 mM cultures, the control and 0.1 mM PLP added at the start of cultivation. In both cases 0.01 mM PLP results in higher growths while 1 mM PLP when added from the beginning seems to affect slightly the cell growth.

However, no such findings have been found so far. Still, the mechanism that PLP is transported intracellularly is unknown. Initially PLP was thought to be membrane-impermeable and only the uptake of non-phosphorylated forms of vitamin B<sub>6</sub> was recorded (Dempsey and Pachler, 1966). However, in their work Saxena et al., 2022 suggested that PLP is internalised, and this internalisation achieves the stabilization of the PLP-dependent enzyme. That is why the later supplementation point was examined, as it allows some time for the PLP to diffuse to the inside of the cells, while the incubator cools down. Although these observations, the differences between the conditions tested are quite small and more replicates are needed to draw conclusions.

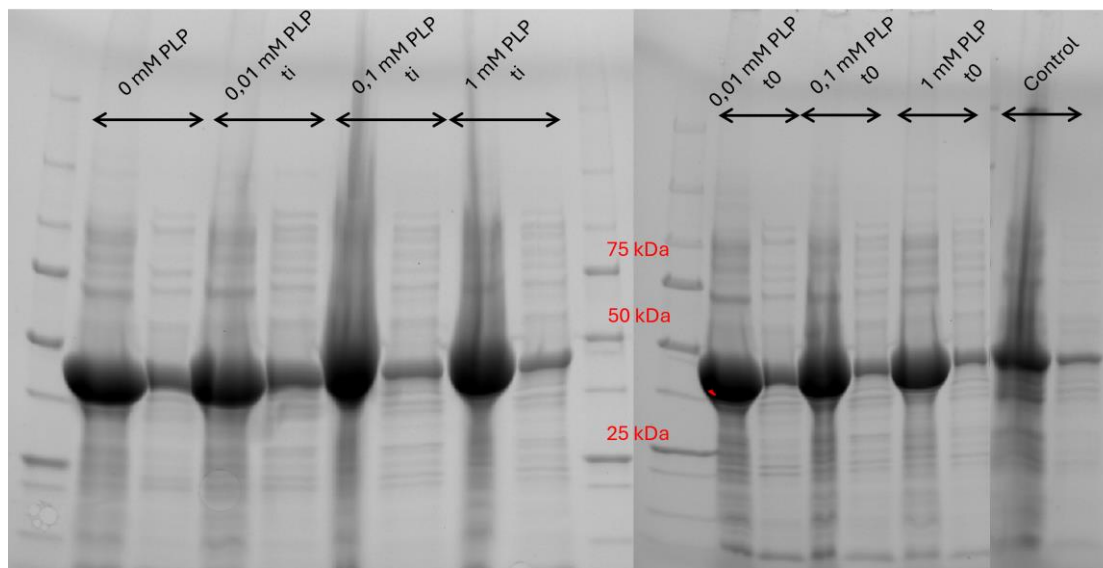


**Figure 6 SDS-PAGE of samples after extraction.** For each culture, a sample of total fraction (TF, left) and soluble protein fraction (SF, right) is run. Only the second replicate is presented here. Same sample volumes have been loaded. The expression of recombinant protein is pronounced across all conditions. Yet, in all cases the soluble ATA-10 roughly represents about 20% of the total fraction. Interestingly, in the control samples a band of 50 kDa can be observed.

The solubility of the recombinant ATA-10 was assessed with densitometry (Figure 6). The data show no difference in the target protein yield in the soluble protein fraction for all the different PLP supplementation conditions. In all cases, the soluble ATA-10 represents approximately 60% of the soluble protein fraction and 20% of the total protein fraction. This is further observed by the total protein concentration and enzyme concentration of the different conditions presented in Figure 7A. The total protein concentration of the soluble protein fraction is rather randomised under different PLP concentrations. However, the supplementation time of PLP affects the target protein yield in the soluble protein fraction. In both replicates, soluble protein fractions where PLP was added from the beginning of the culture result in lower overall total soluble concentration than cultures with PLP added before induction. These findings support our hypothesis that supplementation of PLP during growth has a beneficial role in protein solubility. However, they are not consistent with the findings of Saxena et al., 2022. In this study, PLP supplementation of 0.01-0.1 mM led to a 4.2-18% increase in target protein yield in the soluble protein fractions, respectively. Also, statistically non-significant differences were

observed in the cases where the induction was carried out at 16 °C overnight, an induction that is more similar to the one carried out in this report. The specific productivity for the tested conditions was also calculated (Figure 14, Appendix). The values varied between 0.7-2.0 mg ATA-10/g cells/L/h and followed the same trend as the total soluble protein concentration.

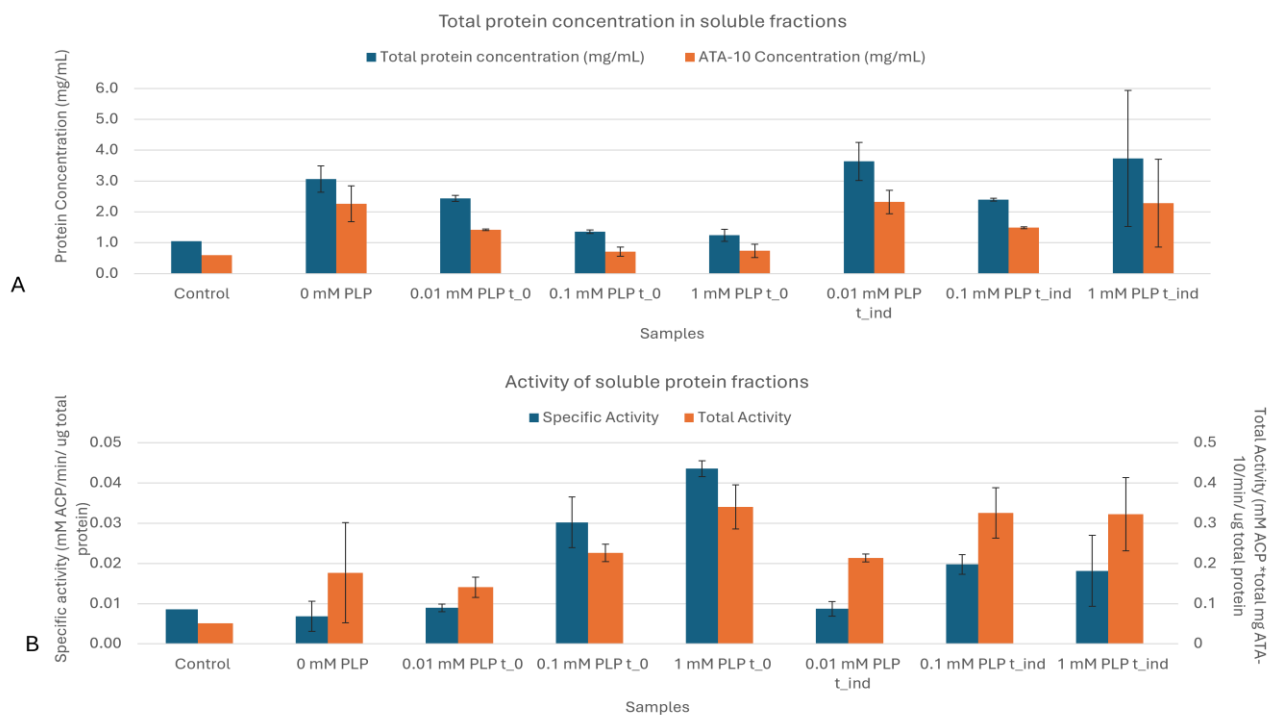


**Figure 7 Protein and activity analysis of the soluble protein fractions (SF).** Top: Total protein and ATA-10 concentrations in the soluble protein fractions. The results represent the average of two replicates. The total protein concentration seems to be stochastic, rather than affected by the PLP concentrations. PLP seems to affect though the total solubility yields negatively when added from the beginning of cultivation. However, the ATA-10 concentrations remain stable across all conditions in respect to the total protein concentrations of the SF. Bottom: Specific activity (blue) and total activity (orange) yield measured in the soluble protein fractions. The results represent the average of two replicates. Here, the activity is increasing linearly with regards to the PLP concentration. PLP added from the beginning of the cultivation leads to higher specific activity although lower protein concentration, implying assistance in enzyme folding. Total activity is comparable for samples with 1 mM PLP at both times of addition and 0.1 mM PLP supplemented at t(i).

The activity of the recombinant ATA-10 in the soluble protein fraction was also assessed, and the results are presented in Figure 7B. It is evident that the addition of PLP leads to increased specific activity. Particularly, by increasing the PLP concentration in the growth medium the specific activity increases linearly. It should be noted that for both replicates, the soluble protein fractions where PLP was supplemented at the beginning of the cultivation, yield higher activity. ATA-10 in soluble protein fraction with 0.1 mM PLP t<sub>0</sub> and 1 mM PLP t<sub>0</sub> result in 3-fold and 4-fold increase in activity, respectively. This is an interesting observation given that the target protein yield in the soluble protein fractions with PLP supplemented at t<sub>0</sub> is overall lower than the soluble protein fractions without PLP. More specifically, the trend of increased activity is opposite to the trend of decreasing protein concentration in these soluble protein fractions (t<sub>0</sub> set). That can be attributed to a better folding of the enzyme when PLP is added from the beginning of the cultivation. PLP has been previously reported to facilitate the protein folding



of PLP-dependent enzymes, however the mechanism largely varies (Livanova et al., 2002, Cai et al., 1995). Interestingly, the total activity of the soluble protein fractions containing 1 mM PLP at both  $t_{(0)}$  and  $t_{(i)}$  and 0.1 mM PLP at  $t_{(i)}$  is comparable. Yet, 1 mM PLP  $t_{(0)}$  has the highest total activity as well.

Surprisingly, an intense band corresponding to the target ATA-10 band was also observed in the case of no induction. For that soluble protein fraction the total protein concentration is on the lower range of what was recorded, and the calculated ATA-10 concentration results from the densitometry performed based on that band (Figure 7A). The specific activity of that sample was also at low levels, comparable to samples with induced expression (Figure 7B). To investigate if this protein is the recombinant ATA-10 the sample was purified and the activity of the eluate was measured (Figure 15, Appendix). The eluate has a faint band to where the ATA-10 is expected, but the intensity of this band is approximately the same as a band of similar MW in the flowthrough. The specific activity of the eluate shows very low activity, which, however, is 20 times higher than the native *E. coli* activity on the same culturing conditions (Specific activity measured on soluble protein fractions of *E. coli* (pET22b) = 0.00009 mM ACP/min / $\mu$ g total protein). Combining the results from electrophoresis and activity test, we preliminary conclude that this protein is a native *E. coli* protein of 50 kDa that shows affinity towards the resin. Further investigation should be made to clarify if there is leaking expression or a native protein. MS-protein fingerprinting is a valuable tool that could allow such analysis.

### 3.2.1. Purification of ATA-10 from soluble protein fraction

Several samples of recombinant ATA-10 were purified with nickel-affinity chromatography to examine the stability of the pure enzyme. The complete chromatogram from the purification of one soluble protein fraction containing 1 mM PLP at  $t_{(0)}$  is presented in Figure 8A and the samples from that purification process were electrophoresed as shown in Figure 8B. Recombinant enzyme demonstrated comparatively high affinity to chromatography resin even with single-step affinity chromatography. However, one main limitation observed during the purification of soluble protein fractions containing PLP was the interference of PLP with the protein UV absorbance. During affinity chromatography the binding and elution phase are indicated through rise in the UV absorbance values. As PLP naturally absorbs in the UV spectrum, the protein detection is masked.

In the example of soluble protein fraction with 1 mM PLP  $t_{(0)}$ , the two elution fractions accounted for 0,577 mg/mL and 1,389 mg/mL, respectively. The second eluate showed aggregation even after one day of storage at 4 °C. To concentrate the pure enzyme solution, the two samples were first filtered and then combined, with a final concentration of 0,77 mg/mL. Due to technical factors concerning the concentration process, the concentration was performed twice with final concentration of pure enzyme 0,41 mg/mL with a specific activity of 0,009 mM ACP/min/ $\mu$ g total protein. This activity is only 18,1% of the activity measured for the respective



soluble protein fraction. It is likely that the aggregation tempered with the activity of the enzyme.

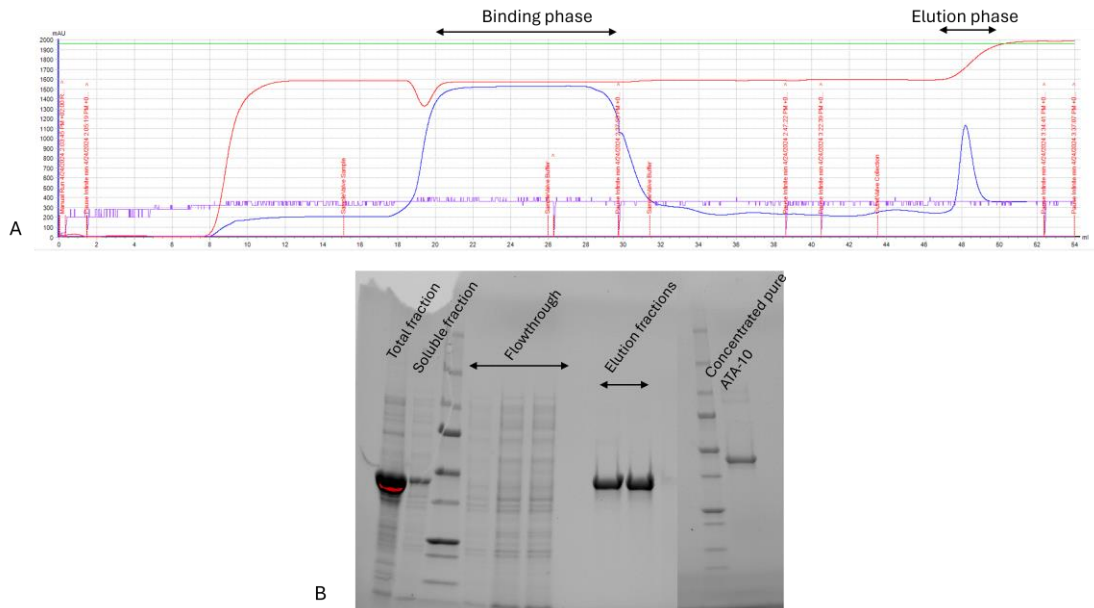


**Figure 8 Purification of recombinant ATA-10 from soluble protein fraction.** In this case soluble protein fraction containing 1 mM PLP  $t_0$  is presented as an example. A: Purification chromatogram. The 1 mM PLP affects the UV absorbance, leading to lower values than expected. B: Electrophoresis of samples before and after purification. On the left the total and soluble protein fraction are presented. The purification procedure yields fairly pure enzyme even after one step of purification. The concentrated sample of pure ATA-10 after filtration of the aggregated solution is run on the right side, with a final concentration of 0,41 mg/mL.

### 3.2.2 Testing limits of PLP supplementation

To test the threshold of PLP supplementation at which a negative effect on transaminase might occur, cultures supplemented with 10 mM PLP at the beginning were carried out as described in section 2.2. It was assumed that if the PLP bears any toxicity on the cell growth that would be more pronounced in the case of longer presence of it in the cell growth environment. **Figure 9A** shows the growth curves of the cultures without and with 10 mM PLP. Both duplicates had similar growth to the control culture until induction, whereas after that the cell growth was almost half of the 0 mM PLP. The results suggest that PLP do not bear any burden on cell growth during growth, but only during induction. The slower growth during induction was also observed for cultures with 1 mM PLP supplemented at  $t_{(0)}$ . The total soluble protein concentration was similar between the two PLP conditions (**Figure 9B**). The soluble ATA-10 concentration was slightly lower in the case of 10 mM PLP, while the specific activity increased 5-fold. This small difference in ATA-10 concentration in the soluble protein fraction could be attributed to limits of protein quantification applying densitometry. This high PLP concentration interferes with the dye resulting in very thick bands, that could lead to inaccurate results (Figure 17, Appendix).

Compared to the rest of the soluble protein fractions where the PLP was supplemented at the beginning of cultivation, although the soluble protein concentration was higher in the presence

of 10 mM PLP, the activity was not much improved. Indeed, the specific activity of the 10 mM PLP soluble protein fraction was almost half of the 1 mM PLP soluble protein fraction and slightly less than the 0.1 mM PLP soluble protein fraction (Figure 7B). ATA-10 was also purified from soluble protein fractions of 10 mM PLP. However, that high PLP concentration prevailed over the UV absorbance of proteins, making the process very complicated (Figure 16, Appendix). The pure enzyme was of low concentration (0.28 mg/mL and 0.19 mg/mL after filtration, Figure 17, Appendix), and it demonstrated aggregation after 1 day storage at 4 °C as well.

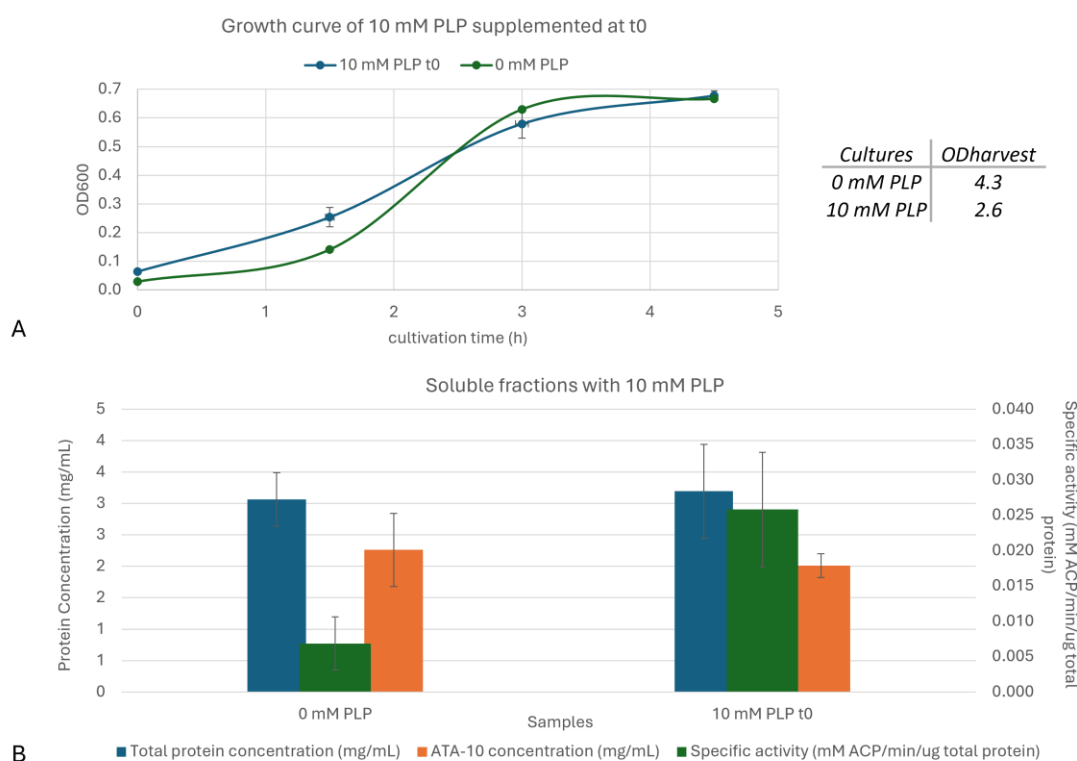


**Figure 9 Growth and soluble protein fraction analysis with 10 mM PLP supplemented from the beginning of the culture.** A: The growth curves of cultures with 10 mM PLP with 1 mM (performed in duplicates) and a control a culture with 0 mM PLP and 1 mM IPTG is used here from the same inoculum. The cell growth in the presence of 10 mM PLP is almost 2-fold lower than without PLP during induction phase but is the same during growth phase. B: Total protein concentration, ATA-10 concentration and activity measured in the collected soluble protein fractions. The solubility yield seems to not be influenced by the addition of 10 mM PLP, but the activity 5-fold increased.

Overall, the results imply the active help of PLP in the ATA-10 folding process rather than the native state stabilization. This is highlighted by differences in activity with varying PLP concentrations and supplementation points, whereas the yield of the target protein remains around 60% in the soluble protein fraction. Yet, aggregation at concentrations above 1.5 mg/mL were observed across all PLP concentrations. Other techniques of improving solubility should be examined. In their work, Kollipara et al., 2022 mention the coexpression of chaperones to optimize the expression of the studied transaminases. Although, these results are not published, it is a strategy commonly employed to improve the solubility yield of heterologous proteins (Gopal and Kumar, 2013). Compiling all observations together, cultivating the recombinant ATA-10 in the presence of 1 mM PLP from the beginning of the culture yielded the best results. The specific productivity of cultivation at 1 mM PLP  $t_{(0)}$  was 0.67 mg ATA-10/g cells/h, which

is approximately half of the cultivation without PLP. The highest productivity values were reported for cultures without PLP and with 0.01 and 1 mM PLP supplemented before induction. The trend of the specific productivity follows the same trend as the total soluble protein concentration, which highlights the importance of improving the yield. For downstream applications and upscale of the process, different practices could be tested to increase the yield and productivity of the recombinant ATA-10. To that direction, high cell density cultivation, reducing the concentration of IPTG and rich media can be tested. Reducing the inducer concentration can facilitate decrease in the protein synthesis rate and a reduction in the number of inclusion bodies (Larentis et al., 2014). Additionally, given that the mechanism of PLP uptake is unknown the supplementation of the non-phosphorylated form, pyridoxine, can be examined as an alternative of cofactor supplementation. For the PLP-dependent glutamate decarboxylase pyridoxine supplementation allowed improvements in stability, yield of active protein and specific enzyme activity (Huang, Su and Wu, 2016).

Previous reports on amine transaminase showed that external supply of PLP can have a positive impact on the transaminase catalysing reactions. Kaulmann et al., 2007 reported addition of 0.25 mM PLP led to 2-fold increase in product formation  $\omega$ -TA from *C. violaceum* and highest conversion efficiency with the commercial *V. fluvialis*  $\omega$ -TA. On the other hand, the tetrameric *Pseudomonas* sp. ATA showed increased stability when PLP was externally supplemented up to 10 mM, but the transamination activity was reduced (Börner et al., 2017). One could argue that the reported increase in activity of recombinant ATA-10 could be a result of increased concentration of PLP in the soluble protein fraction, rather than a direct effect on the folding of the enzyme in the host cell. The substrate of the enzyme activity assay contains 2 mM PLP, thus the effect of 10-100  $\mu$ L of 0.01 to 1.0 mM PLP containing samples in 1 mL reaction volume should be negligible. However, this concept could explain the lower activity recorded for 10 mM PLP containing soluble protein fractions (Figure 9B). It would be interesting to explore the effect of PLP on activity, by having soluble protein fractions of varying PLP supplementation lysed in buffers both containing PLP and without PLP. In that direction, an assay that could monitor the PLP diffusion inside the cells would help elucidate the degree of PLP presence during ATA-10 expression.

### 3.3. Immobilization – Stability of enzyme

#### 3.3.1. Initial screening of beads

The stability of the enzyme has proven to be quite challenging so far. A way to try to tackle that problem was decided to be through immobilization on carrier support. For that reason, two different beads were investigated: beads of polyacrylic acid and beads of cellulose. Initially, a screening to examine the degree of binding and activity of the immobilized enzyme on the different beads was carried out. Using the soluble protein fraction collected where PLP was added at the start of cultivation, the samples were mixed with beads with a loading of 19  $\mu$ g of ATA-10/mg beads for soluble protein fraction with 0.01 mM PLP, 21.9  $\mu$ g of ATA-10/mg beads for SF with 0.1 mM PLP and 35.7  $\mu$ g of ATA-10/mg beads for SF with 1 mM PLP. Two different

conditions of immobilization were first tested. One immobilization, following the guidelines of the supplier, was carried out statically at 4 °C for 3 h. The second immobilization was aimed to provide better mixing and was carried out on a nutator plate at RT for 40 h. The results are presented in **Figure 10** and **Figure 11**, respectively.

As can be seen in **Figure 10A**, the shorter immobilization had overall a small protein immobilization yield. The polyacrylic beads resulted in a 2-fold higher degree of immobilization compared to the cellulose beads. Since the activity of the non-immobilized fraction after the immobilization for this screening test is not available, the activity of the immobilized enzyme can only be assessed through the two-phase reactions where MPPA was measured (**Figure 10B**). The activity of the immobilized ATA-10 follows the same trend as the free enzyme, that is having increased activity with increasing concentrations of PLP. Moreover, the immobilized ATA-10 on polyacrylic beads leads to a higher specific activity compared to the ATA-10 immobilized on the cellulose beads. This difference was more pronounced for the 1 mM PLP sample.

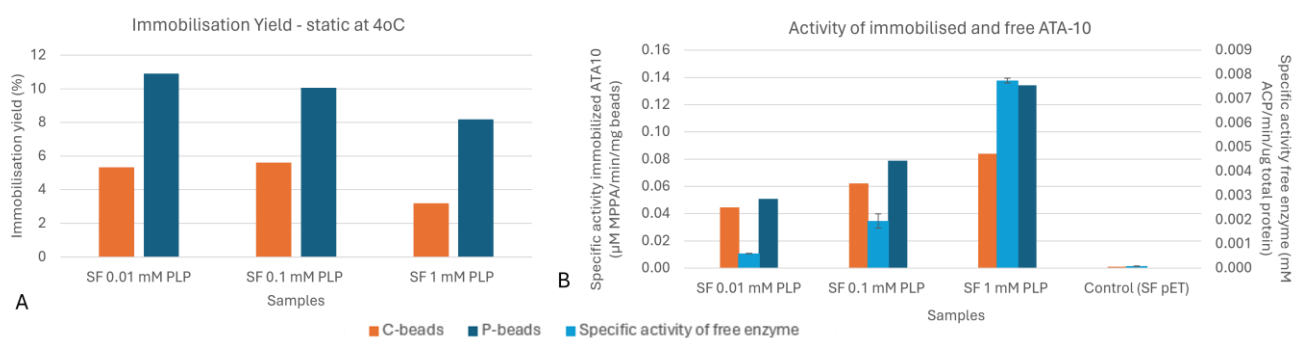


**Figure 10 Screening immobilization for 3 hours at 4 °C.** *A: Immobilization yield calculated for cellulose (C-beads; orange) and polyacrylic acid (P-beads; blue) beads. Overall, the yield is low, but the polyacrylic acid beads show a higher degree of protein binding, almost 2-fold higher than cellulose beads. B: Activity of immobilized ATA-10 on cellulose and polyacrylic acid beads. Since the specific activity of the non-immobilized fraction is not available and the activation yield cannot be calculated, the specific activity of the respective free enzyme is also apposed (light blue). The increasing activity with increasing PLP concentration is also observed here, with the immobilized ATA-10 on polyacrylic acid beads yielding higher activity.*

Similar results were obtained for the screening test of longer incubation at room temperature on a nutator plate. The 40-h immobilization led to higher immobilization yield compared to 3 h immobilization, with the cellulose beads having a smaller immobilization yield compared to the polyacrylic ones (**Figure 11A**). However, the obtained immobilisation yields exhibit some anomalous values, including negative yields and yields exceeding 100%. Firstly, the immobilization yield of SF 1 mM PLP on cellulose beads has a negative value of -6.07%. A reasoning that could explain this negative value is that there could have been some aggregation in the SF 1 mM PLP before the immobilization and the prolonged mixing helped break down these aggregates. In that way, the total protein concentration could have been higher as more protein molecules are available for the Commassie Brilliant Blue G-250 to bind to. This can be further supported by the activity of the bound ATA-10 from that sample shares the same activity

with the rest of the bound enzyme on cellulose beads (Figure 11C) and the activity yield is also close to 100% (Figure 11B). The reason why this was not observed at the first screening test (Figure 10) can be credited to the longer immobilization time or the better mixing that allows more interactions between proteins without HIS-tag and carriers.

Moreover, the immobilization yield of the polyacrylic acid beads, although much higher than the cellulose ones, exceeded 100% (Figure 11A). That would mean that the bound protein on the carrier was higher than the available free transaminase. Again, that could be a result of entrapment of protein aggregates that were broken down due to the prolonged incubation on nutator plate. Interestingly, considerable amount of bound protein (1710,2  $\mu\text{g}$ ) on the polyacrylic acid beads was also observed for the control soluble protein fraction. The control soluble protein fraction has no transaminase expression, which has been previously validated by both activity assay and imaging with SDS-PAGE. To add to that, the activity of the immobilized protein for the control sample is marginal, 50 to 100 times lower than the rest of the immobilized ATA-10 on polyacrylic acid beads (Figure 11C). These observations suggest that the bound proteins aren't the target enzyme, and probably stems from a non-specific binding or hydrophilic interactions between hydrophilic beads and proteins in the lysate. The soluble protein fractions contain a wide variety of intracellular soluble proteins and 50 mM imidazole that could potentially interact and bind to the polyacrylic acid beads. Given the diversity of the solution it cannot be specified what binds to them. Based on Table 1, the polyacrylic acid beads have lower Ni loading than the cellulose beads, which one would expect to result in more competitive binding. Also, the high activity yield obtained for the control soluble protein fraction on cellulose beads should not be considered, as the activity of both the soluble protein fraction and the non-immobilized fraction are almost null.

By subtracting the bound protein value of the control from the rest of the samples, the immobilization yield for the polyacrylic acid beads is normalized, which further supports the idea of non-specific binding (Figure 11A). Even in that case, the immobilization yield of the polyacrylic acid beads is higher than the cellulose beads, with an exception for the soluble protein fraction with 0.01 mM PLP. This subtraction also entails assumptions; thus, it cannot be trusted either. For instance, the samples with expressed ATA-10 have more competition for correct binding to the carrier than the control sample. Thus, it cannot be certain if the degree of non-specific binding is the same across all samples and if the above subtraction leads to accurate values. The general trend suggests that polyacrylic acid beads result in higher immobilization yield than the cellulose ones.

For the polyacrylic acid beads the longer immobilization also resulted in halved activity of the immobilized protein (Figure 11C). Although the immobilization yield after 40 h was much higher than after 3, the activity of the immobilized enzyme seemed to decrease. The nonspecific binding could potentially temper with the activity of the bound enzyme, as less active sites are available per bead or interactions between the bound proteins occurred. Furthermore, the prolonged immobilization in room temperature could also have played a role in the activity of

the bound enzyme. The activity yield, however, shows that the bound enzyme kept its activity, apart from the 0.01 mM PLP SF. Comparing the activity yields between the two beads the differences here are not that pronounced. The overall trend of higher activity with higher PLP concentrations remains. Yet, this trend does not match the activity of the bound ATA-10. Here, the bound ATA-10 on cellulose beads is similar across all PLP concentrations, independently of the differences on the immobilization and activity yields.

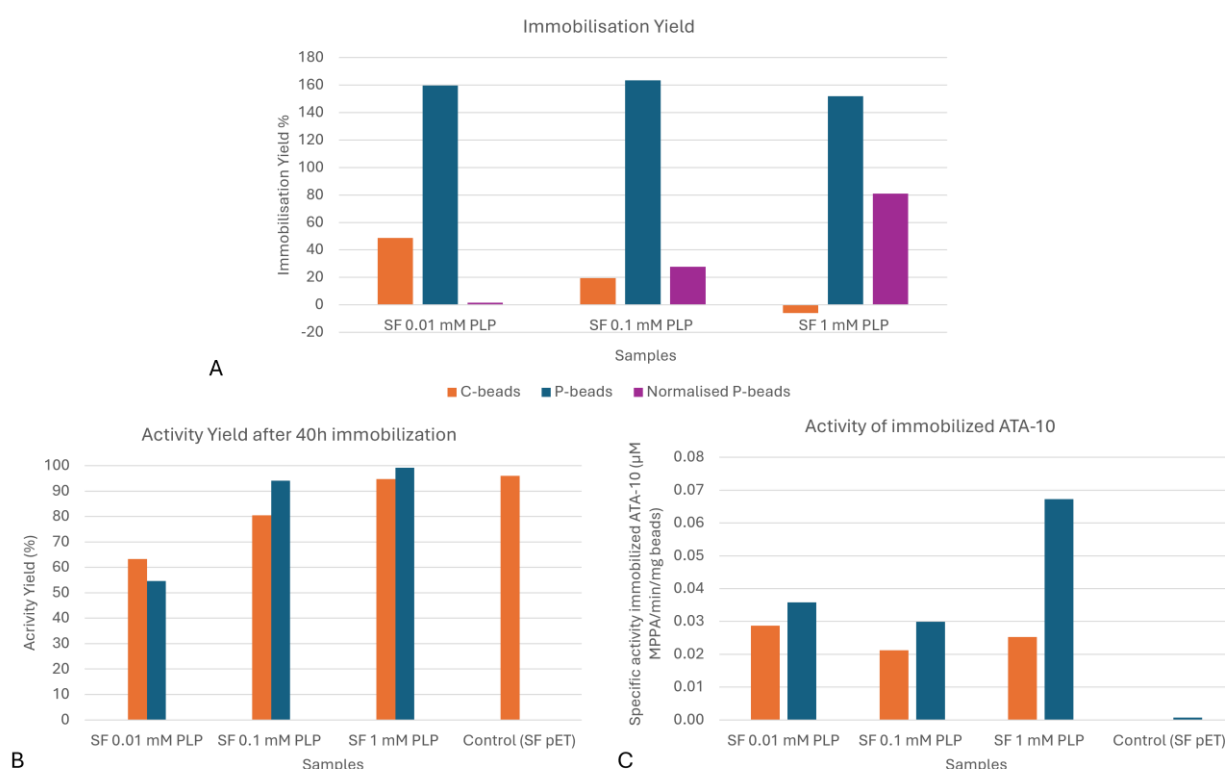


**Figure 11 Screening immobilization for 40 h at room temperature on a nutator plate.** A: Immobilization yield of cellulose (C-beads; orange) and polyacrylic acid (P-beads; blue) beads. Given the yield for P-beads was above 100%, a normalization of the immobilization yield of the P-beads was attempted by subtracting the amount of bound protein recorded for the control sample (purple). B: Activity yield of C-beads and P-beads. The activity yield was lower for the 0.01 mM PLP sample and higher for the 1 mM PLP sample. C: Specific activity of immobilized ATA-10. The immobilized enzyme on P-beads have higher activity than the C-beads. However, the 0.1- and 1-mM samples showed reduced activity compared to the shorter immobilization.

Lastly, the immobilized ATA-10 with 1 mM PLP on polyacrylic beads (3P in Figure 11) was examined for its storage stability after 4-week at 4 °C. The immobilized ATA-10 retained only 1.64% of its activity (Figure 18). However, the immobilized enzyme was stored in the reaction medium of the two-phase reaction system (2.3.2). This storage condition was not ideal. Product or substrate inhibition maybe have resulted in loss of activity. Immobilized enzymes should be separated from the reaction medium and stored in an appropriate buffer.

### 3.3.2. Testing different immobilization conditions

To investigate whether the temperature and the mixing impacts the activity of the immobilized ATA-10, two different conditions of temperature and mixing were tested. Polyacrylic acid beads showed overall better results in previous experiments, thus they were chosen for this experiment. 40 h long immobilization was carried out i) statically at 4 °C, ii) rotating at RT and iii) rotating at 4 °C. The samples were mixed with beads with a loading ranging between 12,3 and 32,0 µg of ATA-10/mg beads (**Table 4**).

**Table 4** Loading of enzyme on polyacrylic beads for the different samples used.

Soluble protein fraction samples	0.01 mM PLP t <sub>i</sub>	0.1 mM PLP t <sub>i</sub>	1 mM PLP t <sub>i</sub>	0.01 mM PLP t <sub>0</sub>	0.1 mM PLP t <sub>0</sub>	0 mM PLP
Loading (ug ATA-10/mg beads)	32.0	12.6	12.3	24.6	12.3	24.9

This immobilization resulted again in immobilization yields above 100% (**Figure 12A**). The yield between the soluble protein fractions is only slightly different. In agreement with the results of 3.3.1, it appears that even prolonged static immobilization leads to lower immobilization yield, whereas immobilization carried out in room temperature on a nutator plate results in the highest observed yields. This further strengthen the theory that mixing ensures better interactions between the beads and the proteins and potentially low temperatures (4 °C) confine the non-specific interactions to a small degree. Moreover, the activity yield of the different conditions is poorly assessed in this case (**Figure 12B**). That is because the soluble protein fractions had aggregated by the time that the specific activity was measured, therefore the recorded values are expected to be lower than the initial. Negative activity yield would imply that the calculated activity bound to the carrier is greater than the initial total enzyme activity measured before immobilization. That could be true in the case of aggregates in the soluble protein fraction used that broke down during the long immobilization, given that aggregated enzyme has lower activity than the free tetramer. Despite that, what can be observed is that in most cases the activity of the non-immobilized fraction of immobilizations performed at 4 °C give lower values, indicating that the lower temperature prevents loss of activity in such long incubation times.

A more accurate comparison of the effect of the different immobilization conditions could be made by the specific activity of the bound ATA-10 on polyacrylic carriers (**Figure 12C**). In most cases, except for 0.01 mM PLP t<sub>(i)</sub>, stirred immobilization leads to even higher values compared to RT. Moreover, in samples with lower loading immobilization at 4 °C with stirring yields elevated activity. Notably, 0.1 mM PLP t<sub>(i)</sub> demonstrates a 2-fold increase in activity when immobilized at 4 °C with stirring. All samples but one (0.01 mM PLP t<sub>(i)</sub>) have a slightly smaller activity after static immobilization. These results could highlight a trend of better activity after immobilization at 4 °C with stirring, however more replicates need to draw conclusions.



The lower activity observed in 3.3.1 for 40 h immobilization at RT (Figure 11C) was initially thought to be affected by the immobilization temperature. Immobilization with stirring at 4 °C for 40 h (Figure 12C) do not show major increase on the activity of the bound ATA-10. In addition, the activity after static immobilisation after 40 h being half than the ones after 3 h. These results imply that eventually the temperature was not the main factor that decreased the activity, but the immobilization time. It should be noted that the activity of the bound enzyme from different samples is heavily influenced by the loading. Samples 0.01 mM PLP t<sub>i</sub>, 0.01 mM PLP t<sub>0</sub> and 0 mM PLP that had higher loading (Table 4) lead to higher overall specific activities.

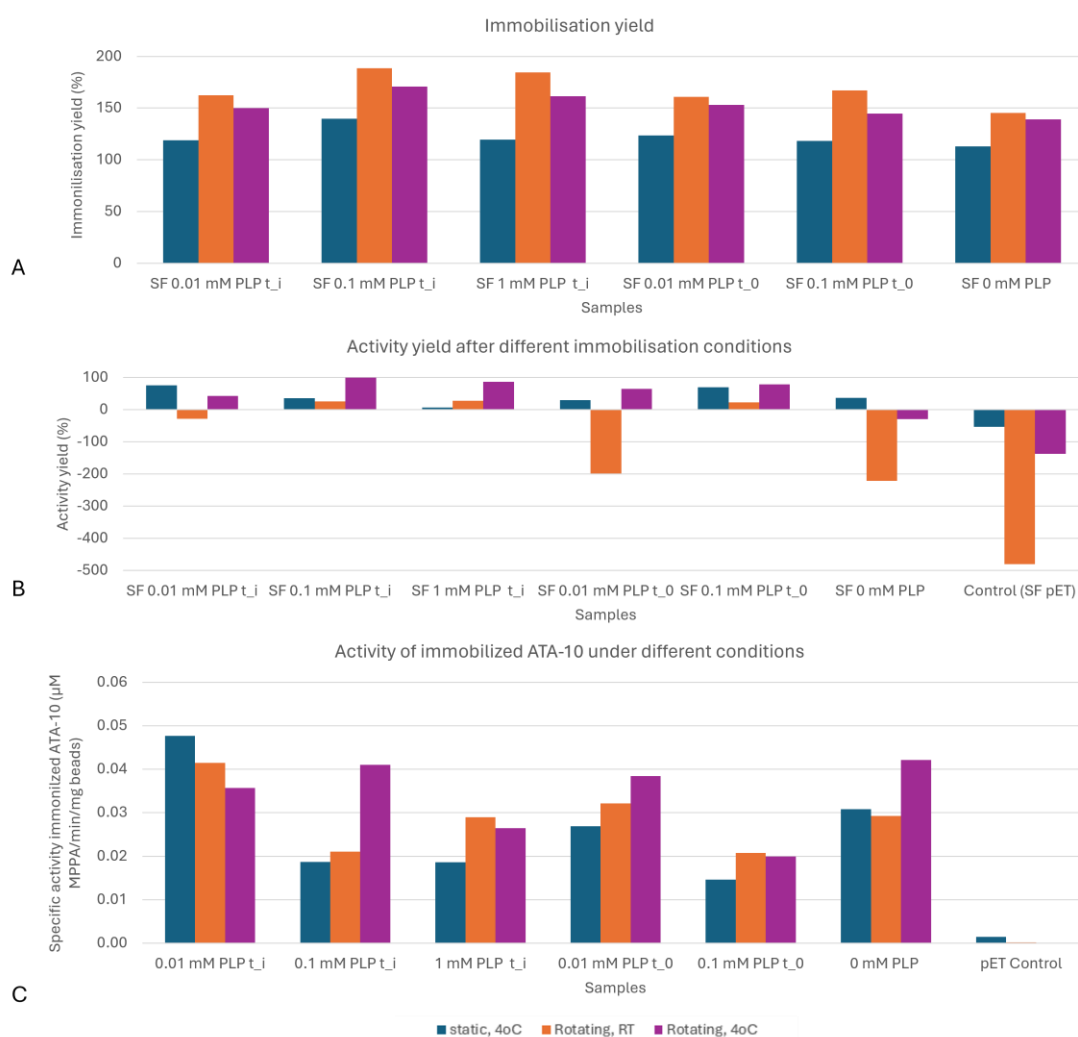


**Figure 12 Immobilization on polyacrylic acid beads under different temperature and mixing conditions.** Immobilization carried out statically at 4 °C; blue, on a nutator plate at RT; orange and on a nutator plate at 4 °C; purple. **A:** Immobilization yield. The yield exceeded 100%. The static immobilization and the immobilization at room temperature recorded the lowest and the highest values, respectively, across all samples. **B:** Activity yield of immobilization. Negative values and fluctuations are observed, most likely due to the soluble protein fractions having aggregated by the time their specific activity was assessed. **C:** Specific activity of immobilized ATA-10 on polyacrylic acid beads under different immobilization conditions.



Immobilization is a common strategy to improve the stability of transaminases. The obtained results show that immobilization on the polyacrylic carriers is successful with high yields. However, more batches need to be carried out to achieve optimization. Temperature, protein loading, immobilization time all play a role in improving the immobilization of ATA-10. Simultaneously, immobilization can serve purification purposes. Lastly, different carriers could be explored for the immobilization of ATA-10. Site-specific immobilization enables targeted immobilization and can avoid detrimental binding. Thus, utilizing the HIS-tag of the ATA-10 on other carriers could lead to advantageous results. Recently, a recombinant of CvTA was simultaneously isolated and immobilized by binding on silica nanoparticles (SNPs) with Ni affinity linkers where a two-fold decrease in enzymatic activity was observed when the immobilization was done with the purified CvTA instead of the crude cell extract (Gábor Koplányi et al., 2023).

## 4. Conclusions

In this report, the ATA-10 from *Burkholderia multivorans* CGD1 (B9AZ94) was successfully cloned and expressed in *E.coli* under varying PLP concentrations. Immobilization was employed to stabilize the transaminase for downstream production processes.

1. PLP concentrations varying from 0.01 to 1 mM PLP do not show burden towards cell growth independently of the time of addition to the growth medium. Small differences are only observed in the growth for samples where PLP was supplemented from the start ( $t_{(0)}$ ). Cultures with 0.01 mM PLP demonstrated cell growth higher than without PLP and 1 mM PLP slowed down the growth. On the other hand, cultures with 10 mM PLP supplemented at  $t_{(0)}$  had similar to the control growth, but after induction the final OD was halved. This could potentially highlight a burden on the cell growth at elevated PLP concentrations that is more pronounced at non-ideal growth conditions (induction performed at 20 °C).
2. The yield of the target protein in the soluble protein fraction remained the same across all different PLP conditions, accounting for 60% of the soluble protein fraction. On the other hand, the total protein was decreased for samples supplemented with PLP at the beginning of the cultivation. A positive impact of PLP was observed for the specific activity measured on the soluble protein fractions. Increasing PLP concentrations led to respective increase of specific activity, in both supplementation times. In addition, soluble protein fractions that had PLP added at  $t_{(0)}$  had overall higher activity than the  $t_{(i)}$  soluble protein fractions. Specifically, 0.1 and 1 mM PLP  $t_{(0)}$  demonstrated 3-fold and 4-fold increase in activity, respectively. The conclusion was made of a possibility that PLP, when supplemented from the beginning of the culture, has a greater effect on the stability of the ATA-10 possibly aiding in proper protein folding. In this context, 1 mM PLP added from the start of the culture is found to be the best condition for heterologous expression of ATA-10 in *E.coli* BL21 (DE3).

3. The stability of the enzyme in soluble protein fraction and after purification proved to be quite challenging. It was observed that the enzyme tends to aggregate in concentration above approximately 1–1.5 mg/mL. Purification of the recombinant ATA-10 on nickel-affinity chromatography was successful even after one step of purification. However, the purification process was largely limited by the PLP presence in the samples. PLP absorbs in the UV spectrum thus impacting the UV signal during the process. The higher the PLP concentration, the weaker the sensitivity of the UV detector for fluctuations in protein concentrations.
  
4. Immobilization of ATA-10 on hydrophilic carriers utilizing the HIS-tag affinity towards Ni<sup>+</sup> was successfully realised. Immobilization on polyacrylic acid beads proved to result in higher immobilization yields and higher activity of the immobilized ATA-10. However, the polyacrylic acid beads showed non-specific interactions with contents in the soluble protein fraction when the immobilization was carried out for 40 h leading to abnormal yields. These interactions were slightly confined when the immobilization was carried out at 4 °C. The prolonged immobilization showed halved activity values compared to the 3h immobilization. Whether the prolonged immobilization promotes non-specific interaction remains to be elucidated. The above results indicate that immobilization at low temperature for more than 3 h could provide better immobilization results.

## 5. References

- Atroshenko, D.L., Sergeev, E.P., Golovina, D.I. and Pometun, A.A. (2024). Additivities for Soluble Recombinant Protein Expression in Cytoplasm of *Escherichia coli*. *Fermentation*, [online] 10(3), p.120. <https://doi.org/10.3390/fermentation10030120>.
- Börner, T., Grey, C. and Adlercreutz, P. (2016). Generic HPLC platform for automated enzyme reaction monitoring: Advancing the assay toolbox for transaminases and other PLP-dependent enzymes. *Biotechnology Journal*, 11(8), pp.1025–1036. <https://doi.org/10.1002/biot.201500587>.
- Börner, T., Rämisch, S., Reddem, E.R., Bartsch, S., Vogel, A., Mark, A., Adlercreutz, P. and Grey, C. (2017). Explaining Operational Instability of Amine Transaminases: Substrate-Induced Inactivation Mechanism and Influence of Quaternary Structure on Enzyme–Cofactor Intermediate Stability. *ACS Catalysis*, 7(2), pp.1259–1269. <https://doi.org/10.1021/acscatal.6b02100>.
- Cai, K., Schirch, D. and Schirch, V. (1995). The Affinity of Pyridoxal 5'-Phosphate for Folding Intermediates of *Escherichia coli* Serine Hydroxymethyltransferase. *Journal of Biological Chemistry*, 270(33), pp.19294–19299. <https://doi.org/10.1074/jbc.270.33.19294>.
- Cho, B.-K., Park, H.-Y., Seo, J.-H., Ju Han Kim, Taek Won Kang, Lee, B.-S. and Kim, B.-G. (2008). Redesigning the substrate specificity of  $\omega$ -aminotransferase for the kinetic resolution of aliphatic chiral amines. *Biotechnology and Bioengineering*, 99(2), pp.275–284. <https://doi.org/10.1002/bit.21591>.
- Compton, S.J. and Jones, C.G. (1985). Mechanism of dye response and interference in the Bradford protein assay. *Analytical Biochemistry*, 151(2), pp.369–374. [https://doi.org/10.1016/0003-2697\(85\)90190-3](https://doi.org/10.1016/0003-2697(85)90190-3).
- de Souza, S.P., Junior, I.I., Silva, G.M.A., Miranda, L.S.M., Santiago, M.F., Frank Leung-Yuk Lam, Dawood, A., Bornscheuer, U.T. and de Souza, R.O.M.A. (2016). Cellulose as an efficient matrix for lipase and transaminase immobilization. *RSC advances*, 6(8), pp.6665–6671. <https://doi.org/10.1039/c5ra24976g>.
- Dempsey, W.B. and Pachler, P.F. (1966). Isolation and Characterization of Pyridoxine Auxotrophs of *Escherichia coli*. *Journal of Bacteriology*, 91(2), pp.642–645. <https://doi.org/10.1128/jb.91.2.642-645.1966>.
- Eliot, A.C. and Kirsch, J.F. (2004). Pyridoxal Phosphate Enzymes: Mechanistic, Structural, and Evolutionary Considerations. *Annual Review of Biochemistry*, 73(1), pp.383–415. <https://doi.org/10.1146/annurev.biochem.73.011303.074021>.

Engelmark Cassimjee, K., Kadow, M., Wikmark, Y., Svedendahl Humble, M., Rothstein, M.L., Rothstein, D.M. and Bäckvall, J.-E. (2014). A general protein purification and immobilization method on controlled porosity glass: biocatalytic applications. *Chemical Communications*, 50(65), p.9134. <https://doi.org/10.1039/c4cc02605e>.

Gábor Koplányi, Bell, E., Zsófia Molnár, Katona, G., Péter Lajos Neumann, Ender, F., Balogh, G.T., Polona Žnidaršič-Plazl, Poppe, L. and Diána Balogh-Weiser (2023). Novel Approach for the Isolation and Immobilization of a Recombinant Transaminase: Applying an Advanced Nanocomposite System. *ChemBioChem*, 24(7). <https://doi.org/10.1002/cbic.202200713>.

Ghislieri, D. and Turner, N.J. (2013). Biocatalytic Approaches to the Synthesis of Enantiomerically Pure Chiral Amines. *Topics in Catalysis*, 57(5), pp.284–300. <https://doi.org/10.1007/s11244-013-0184-1>.

Gopal, G.J. and Kumar, A. (2013). Strategies for the Production of Recombinant Protein in *Escherichia coli*. *The Protein Journal*, 32(6), pp.419–425. <https://doi.org/10.1007/s10930-013-9502-5>.

Grishin, N.V., Konstantin Pervushin and Goldsmith, E.J. (1995). Modeling of the spatial structure of eukaryotic ornithine decarboxylases. *Protein Science*, 4(7), pp.1291–1304. <https://doi.org/10.1002/pro.5560040705>.

Höhne, M. and Bornscheuer, Uwe T. (2009). Biocatalytic Routes to Optically Active Amines. *ChemCatChem*, 1(1), pp.42–51. <https://doi.org/10.1002/cctc.200900110>.

Huang, Y., Su, L. and Wu, J. (2016). Pyridoxine Supplementation Improves the Activity of Recombinant Glutamate Decarboxylase and the Enzymatic Production of Gama-Aminobutyric Acid. *PLOS ONE*, [online] 11(7), pp.e0157466–e0157466. <https://doi.org/10.1371/journal.pone.0157466>.

John, R.A. (1995). Pyridoxal phosphate-dependent enzymes. *Biochimica et Biophysica Acta (BBA) - Protein Structure and Molecular Enzymology*, 1248(2), pp.81–96. [https://doi.org/10.1016/0167-4838\(95\)00025-p](https://doi.org/10.1016/0167-4838(95)00025-p).

Kaulmann, U., Smithies, K., Smith, M.E.B., Hailes, H.C. and Ward, J.M. (2007). Substrate spectrum of  $\omega$ -transaminase from *Chromobacterium violaceum* DSM30191 and its potential for biocatalysis. *Enzyme and Microbial Technology*, 41(5), pp.628–637. <https://doi.org/10.1016/j.enzmictec.2007.05.011>.

Kelly, S.A., Pohle, S., Wharry, S., Mix, S., Allen, C.C.R., Moody, T.S. and Gilmore, B.F. (2017). Application of  $\omega$ -Transaminases in the Pharmaceutical Industry. *Chemical Reviews*, 118(1), pp.349–367. <https://doi.org/10.1021/acs.chemrev.7b00437>.

Kollipara, M., Matzel, P., Sowa, M., Brott, S., Bornscheuer, U. and Höhne, M. (2022). Characterization of proteins from the 3N5M family reveals an operationally stable amine transaminase. *Applied Microbiology and Biotechnology*, [online] 106(17), pp.5563–5574. <https://doi.org/10.1007/s00253-022-12071-1>.

Koszelewski, D., Müller, N., Schrittwieser, J.H., Faber, K. and Kroutil, W. (2010a). Immobilization of  $\omega$ -transaminases by encapsulation in a sol–gel/celite matrix. *Journal of Molecular Catalysis B: Enzymatic*, 63(1-2), pp.39–44. <https://doi.org/10.1016/j.molcatb.2009.12.001>.

Koszelewski, D., Tauber, K., Faber, K. and Kroutil, W. (2010b).  $\omega$ -Transaminases for the synthesis of non-racemic  $\alpha$ -chiral primary amines. *Trends in Biotechnology*, 28(6), pp.324–332. <https://doi.org/10.1016/j.tibtech.2010.03.003>.

Kyratsous, C.A., Silverstein, S.J., DeLong, C.R. and Panagiotidis, C.A. (2009). Chaperone-fusion expression plasmid vectors for improved solubility of recombinant proteins in *Escherichia coli*. *Gene*, 440(1-2), pp.9–15. <https://doi.org/10.1016/j.gene.2009.03.011>.

Larentis, A.L., Nicolau, J.F.M.Q., Esteves, G. dos S., Vareschini, D.T., de Almeida, F.V.R., dos Reis, M.G., Galler, R. and Medeiros, M.A. (2014). Evaluation of pre-induction temperature, cell growth at induction and IPTG concentration on the expression of a leptospiral protein in *E. coli* using shaking flasks and microbioreactor. *BMC research notes*, 7, p.671. <https://doi.org/10.1186/1756-0500-7-671>.

Liang, J., Han, Q., Tan, Y., Ding, H. and Li, J. (2019). Current Advances on Structure-Function Relationships of Pyridoxal 5'-Phosphate-Dependent Enzymes. *Frontiers in Molecular Biosciences*, 6(4). <https://doi.org/10.3389/fmolb.2019.00004>.

Livanova, N.B., Chebotareva, N.A., Eronina, T.B. and Kurganov, B.I. (2002). Pyridoxal 5"-Phosphate as a Catalytic and Conformational Cofactor of Muscle Glycogen Phosphorylase b. *Biochemistry (Moscow)*, 67(10), pp.1089–1098. <https://doi.org/10.1023/a:1020978825802>.

Mallin, H., M Höhne and Bornscheuer, U.T. (2014). Immobilization of (R)- and (S)-amine transaminases on chitosan support and their application for amine synthesis using isopropylamine as donor. *Journal of biotechnology*, 191, pp.32–37. <https://doi.org/10.1016/j.jbiotec.2014.05.015>.

Mathew, S. and Yun, H. (2012).  $\omega$ -Transaminases for the Production of Optically Pure Amines and Unnatural Amino Acids. *ACS Catalysis*, 2(6), pp.993–1001. <https://doi.org/10.1021/cs300116n>.

Oliveira, E.F., Nuno, Fernandes, P.A. and Ramos, M.J. (2011). Mechanism of Formation of the Internal Aldimine in Pyridoxal 5'-Phosphate-Dependent Enzymes. *Journal of the American Chemical Society*, 133(39), pp.15496–15505. <https://doi.org/10.1021/ja204229m>.

Percudani, R. and Peracchi, A. (2009). The B6 database: a tool for the description and classification of vitamin B6-dependent enzymatic activities and of the corresponding protein families. *BMC Bioinformatics*, 10(273). <https://doi.org/10.1186/1471-2105-10-273>.

Plokhov, A.Y., Gusyatiner, M.M., Yampolskaya, T.A., Kaluzhsky, V.E., Sukhareva, B.S. and Schulga, A.A. (2000). Preparation of  $\gamma$ -Aminobutyric Acid Using *E. coli* Cells with High Activity of Glutamate Decarboxylase. *Applied Biochemistry and Biotechnology*, 88(1-3), pp.257–266. <https://doi.org/10.1385/abab:88:1-3:257>.

Rehn, G., Grey, C., Branneby, C., Lindberg, L. and Adlercreutz, P. (2012). Activity and stability of different immobilized preparations of recombinant *E. coli* cells containing  $\omega$ -transaminase. *Process Biochemistry*, 47(7), pp.1129–1134. <https://doi.org/10.1016/j.procbio.2012.04.013>.

Rocha, J.F., Pina, A.F., Sousa, S.F. and Nuno (2019). PLP-dependent enzymes as important biocatalysts for the pharmaceutical, chemical and food industries: a structural and mechanistic perspective. *Catalysis Science & Technology*, 9(18), pp.4864–48 <https://doi.org/10.1039/c9cy01210a>.

Savile, C.K., Janey, J.M., Mundorff, E.C., Moore, J.C., Tam, S., Jarvis, W.R., Colbeck, J.C., Krebber, A., Fleitz, F.J., Brands, J., Devine, P.N., Huisman, G.W. and Hughes, G.J. (2010). Biocatalytic Asymmetric Synthesis of Chiral Amines from Ketones Applied to Sitagliptin Manufacture. *Science*, 329(5989), pp.305–309. <https://doi.org/10.1126/science.1188934>.

Shin, J.-S., Yun, H., Jang, J.-W. ., Park, I. and Kim, B.-G. . (2003). Purification, characterization, and molecular cloning of a novel amine:pyruvate transaminase from *Vibrio fluvialis* JS17. *Applied Microbiology and Biotechnology*, [online] 61(5-6), pp.463–471. <https://doi.org/10.1007/s00253-003-1250-6>.

Sørensen, H. and Mortensen, K. (2005). Soluble expression of recombinant proteins in the cytoplasm of *Escherichia coli*. *Microbial Cell Factories*, [online] 4(1), p.1. <https://doi.org/10.1186/1475-2859-4-1>.

Steffen-Munsberg, F., Philipp Matzel, Sowa, M.A., Berglund, P., Bornscheuer, U.T. and Matthias Höhne (2016). *Bacillus anthracis*  $\omega$ -amino acid:pyruvate transaminase employs a different mechanism for dual substrate recognition than other amine transaminases. *Applied microbiology and biotechnology*, 100(10), pp.4511–4521. <https://doi.org/10.1007/s00253-015-7275-9>.

Toney, M.D. (2005). Reaction specificity in pyridoxal phosphate enzymes. *Archives of Biochemistry and Biophysics*, 433(1), pp.279–287. <https://doi.org/10.1016/j.abb.2004.09.037>.

Toney, M.D. and Kirsch, J.F. (1993). Lysine 258 in aspartate aminotransferase: Enforcer of the Circe effect for amino acid substrates and the general-base catalyst for the 1,3-prototropic shift. *Biochemistry*, 32(6), pp.1471–1479. <https://doi.org/10.1021/bi00057a010>.

Vijay Kumar Saxena, G.V. Vedamurthy and Singh, R. (2022). A novel concept of Pyridoxal 5'-phosphate permeability in E.coli for modulating the heterologous expression of PLP dependent proteins. *Process biochemistry*, 113, pp.37–46. <https://doi.org/10.1016/j.procbio.2021.12.016>.

Yi, S.-S., Lee, C., Kim, J., Kyung, D., Kim, B.-G. and Lee, Y.-S. (2007). Covalent immobilization of  $\omega$ -transaminase from *Vibrio fluvialis* JS17 on chitosan beads. *Process Biochemistry*, 42(5), pp.895–898. <https://doi.org/10.1016/j.procbio.2007.01.008>.



## 6. Appendix

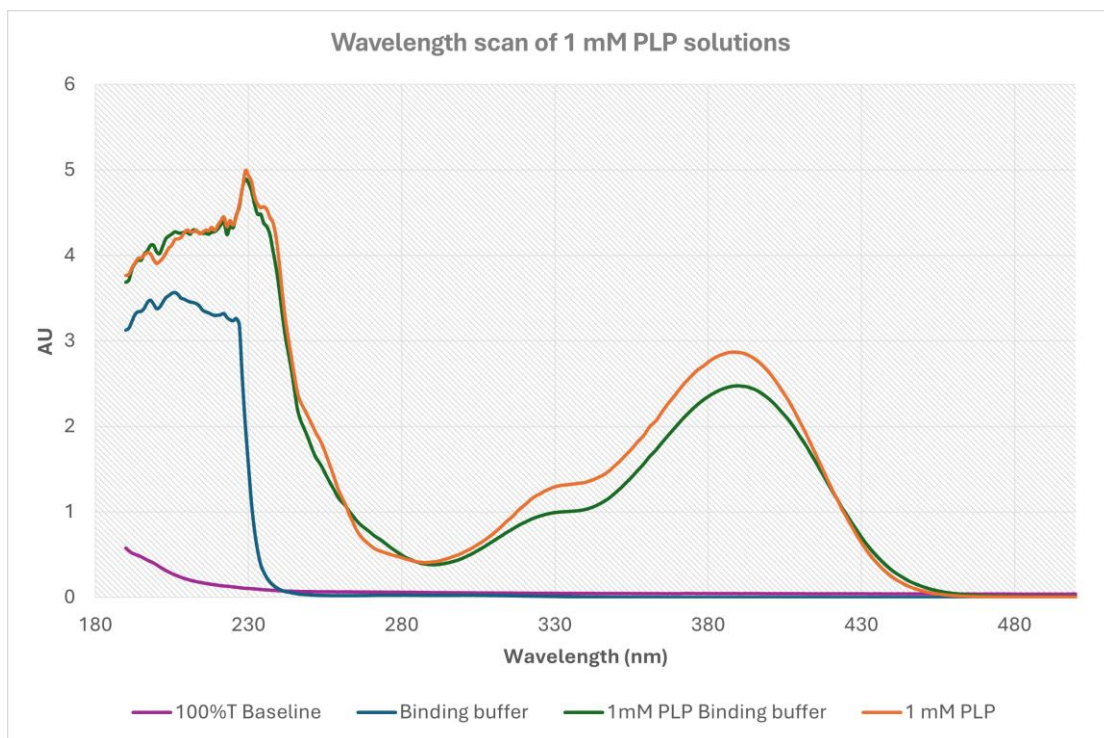


**Figure 13** PLP absorbance wavelength. 1 mM PLP absorbs in the UV spectra which complicated protein concentration measurements and the IMAC procedure.

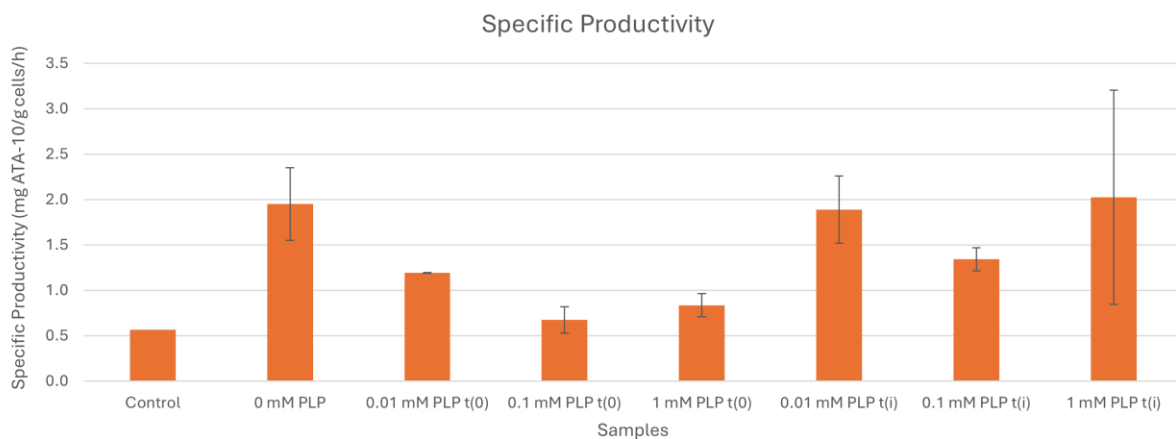


**Figure 14** Specific productivity measured for culture with PLP supplementation. Specific productivity was calculated as the g of ATA-10 produced per g of cells per the hours of the induction phase. The trend of the productivity follows the same trend as the total protein concentration, highlighting the importance of optimizing the yield of the recombinant ATA-10 in the soluble protein fraction. The biomass was calculated on the assumption that 1 OD600 unit equals to 0.5 g cell dry weight/L.



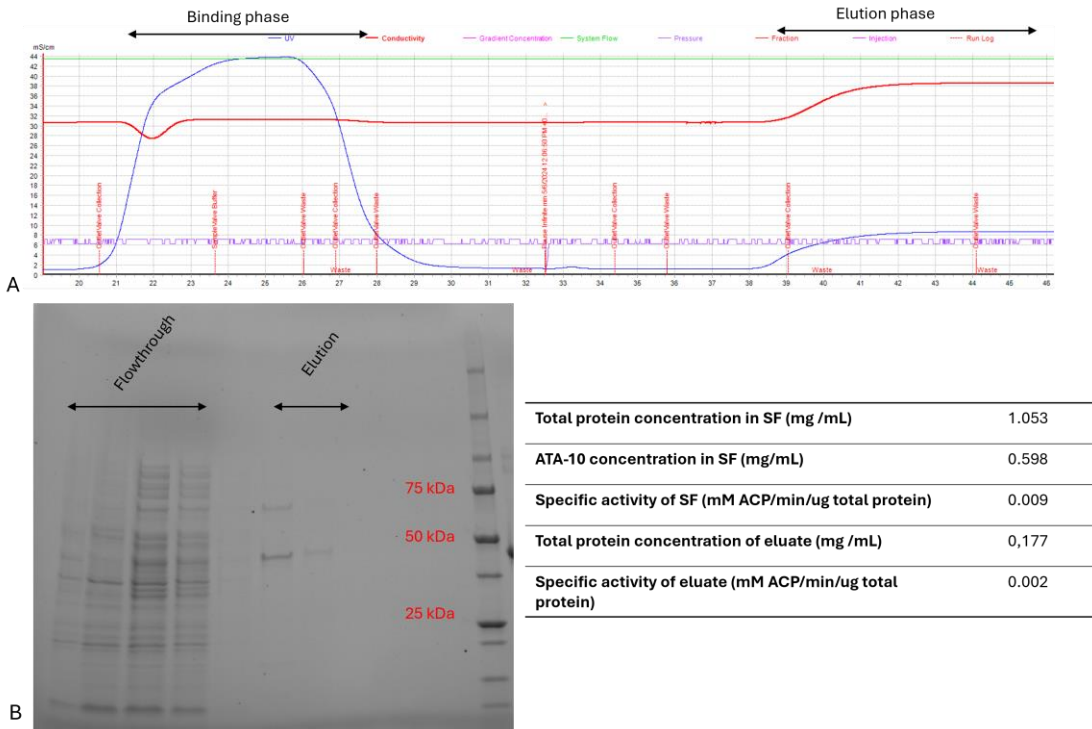


**Figure 15 Investigating the expression of recombinant ATA-10 in samples without induction.** A: Purification of the control sample (no IPTG) with IMAC. The UV signal was significantly low during elution, perhaps hinting at low protein concentration. B: Electrophoresis of purification samples. Flowthrough samples have a faint band of MW similar to the ATA-10, which could be a native E.coli protein. However, the eluates have a faint band of the same MW as the ATA-10. The eluate sample had a concentration of 0.177 mg/mL and specific activity of 0.002 mM ACP/min/ug total protein. This activity is 20 times higher than the native activity of E.coli (Specific activity of the transformation positive control E.coli (pET22b) = 0.00009 mM ACP/min/ug total protein under same culture conditions).

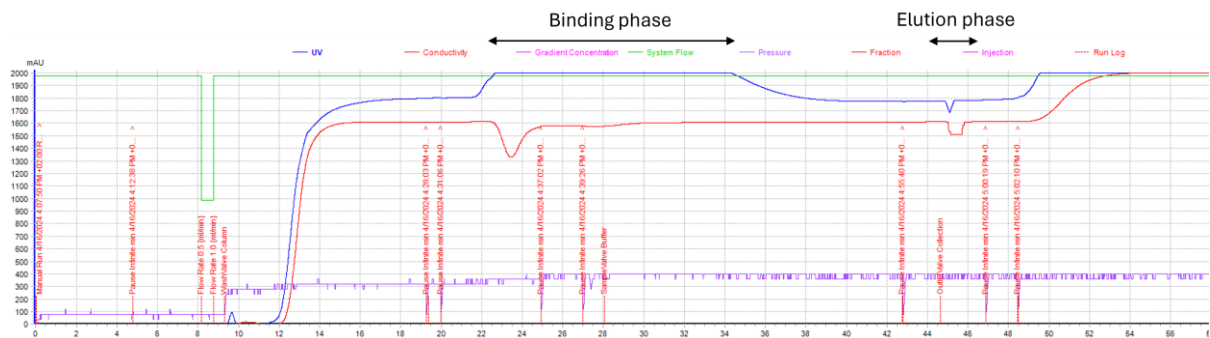


**Figure 16 Ni- affinity purification of ATA-10 from 10 mM PLP soluble protein fraction.** The UV signal remains high throughout the process and the elution is characterized only by a small dip in the UV lasting a mere minute.

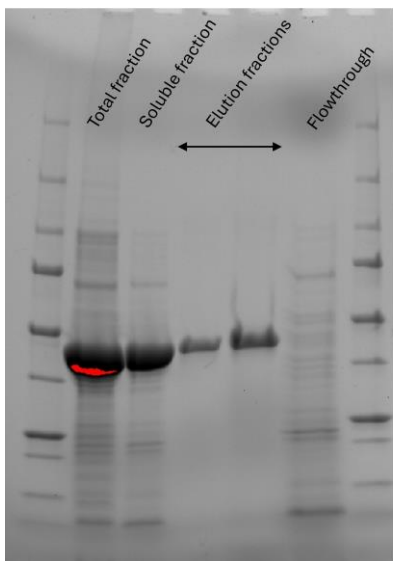


**Figure 17** Electrophoresis of ATA-10 with 10 mM PLP before and after purification. In the total and soluble protein fraction the band intensity is interfered by the high PLP concentration, rendering the densitometry difficult. The elution fractions of the target ATA-10 in 10 mM PLP elution buffer showed aggregation after 1 day storage at 4 °C, with concentrations of 0.28 mg/mL and 0.19 mg/mL after filtration.

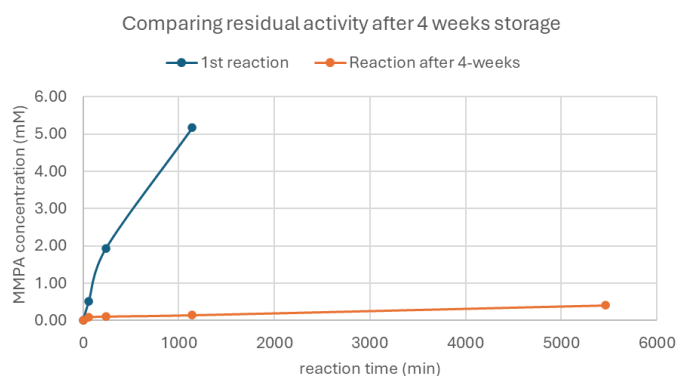


**Figure 18** Storage stability of immobilized ATA-10. The immobilized ATA-10 that showed the highest activity was tested again after 4-weeks storage at 4 °C. The residual activity is only 1.64%. However, the immobilized enzyme was stored in the reaction medium, that could have impaired the activity of the enzyme based on substrate/product inhibition.